

# APPENDIX A: HISTORICAL HYDROGRAPHIC SURVEYS

SOURCE: WATSON, 2008

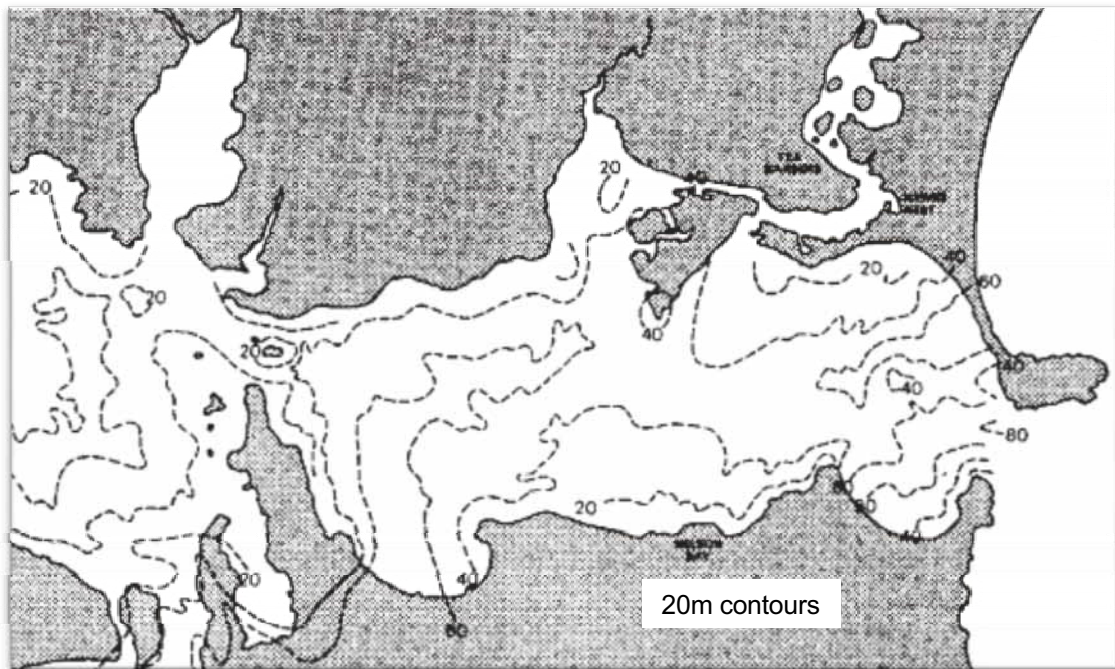
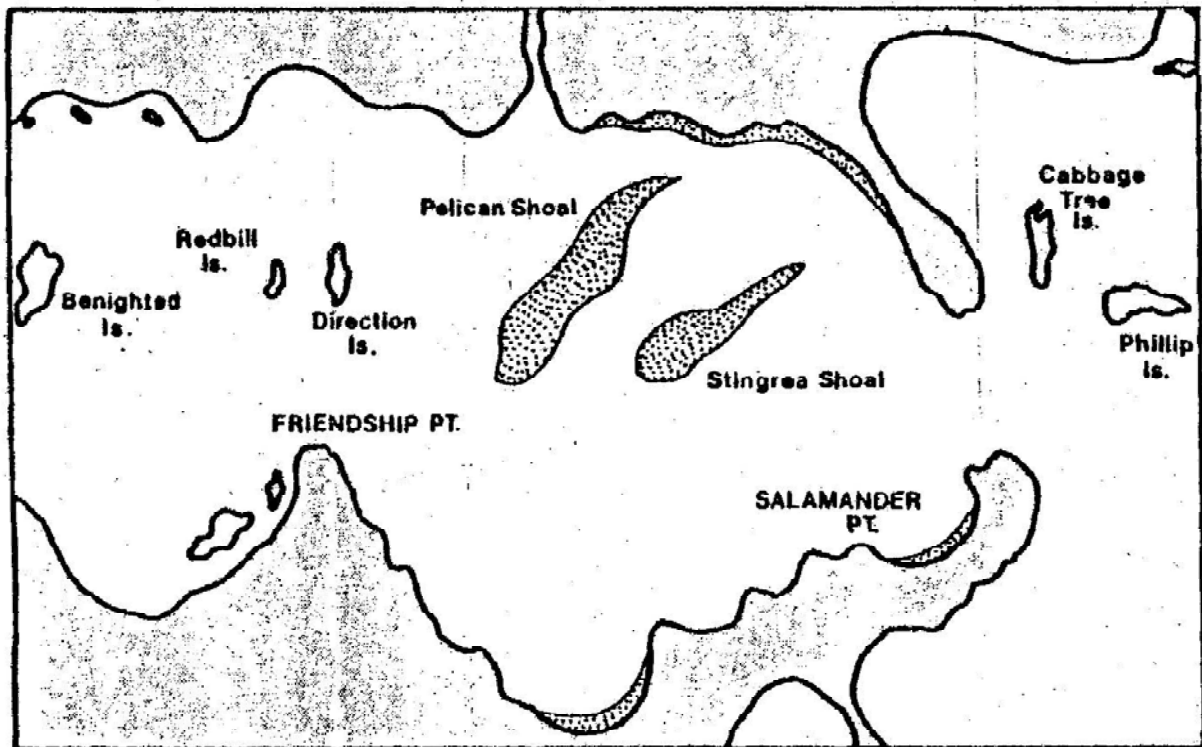
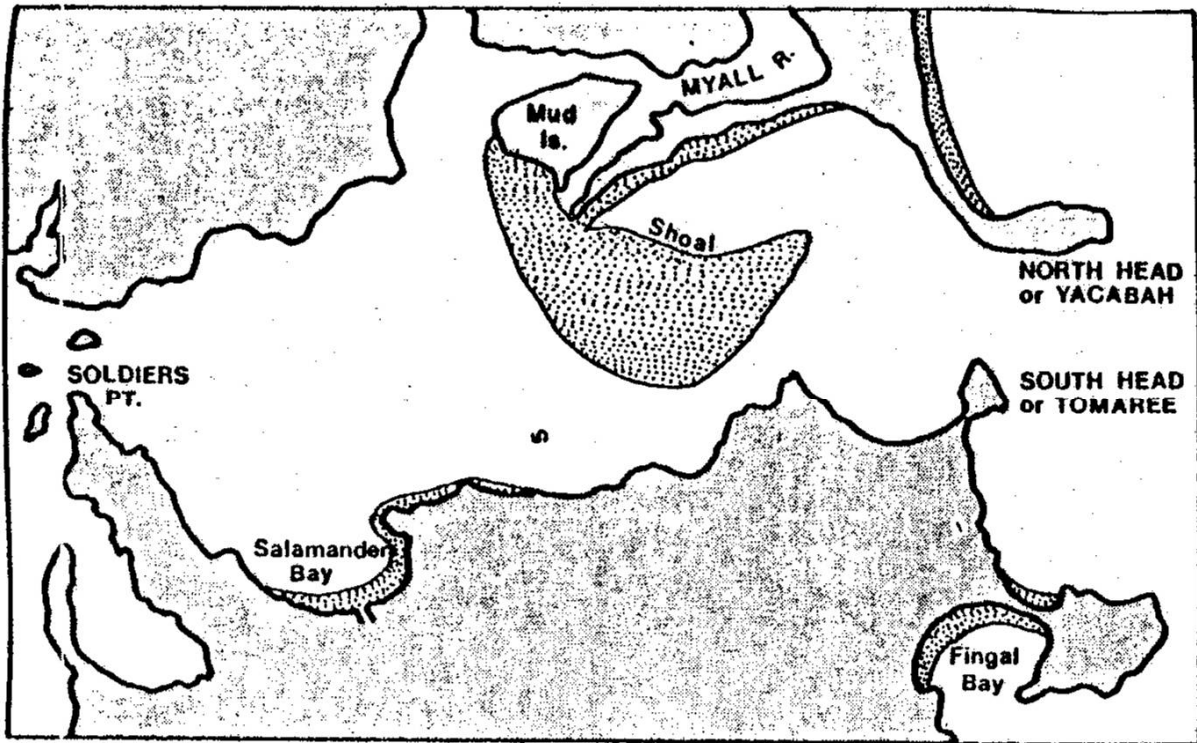


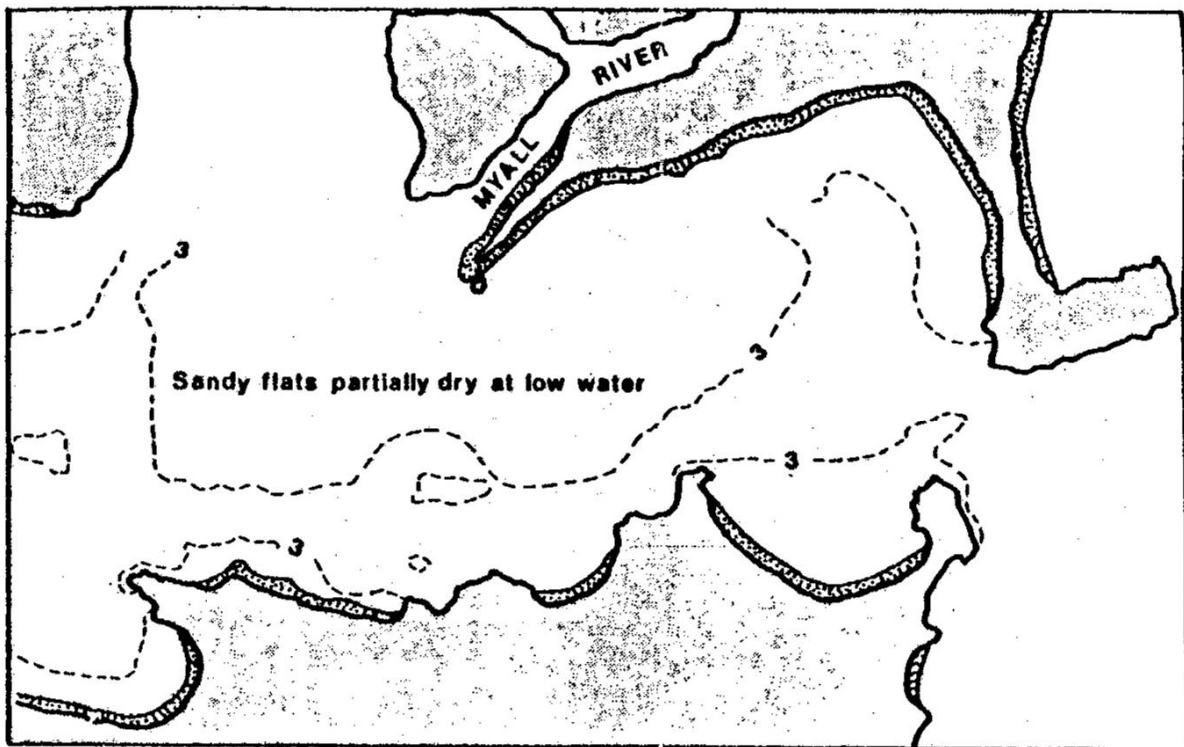
Figure A-1 Bedrock Topography of Port Stephens Source: Thom et al 1992



1792 - WATLING

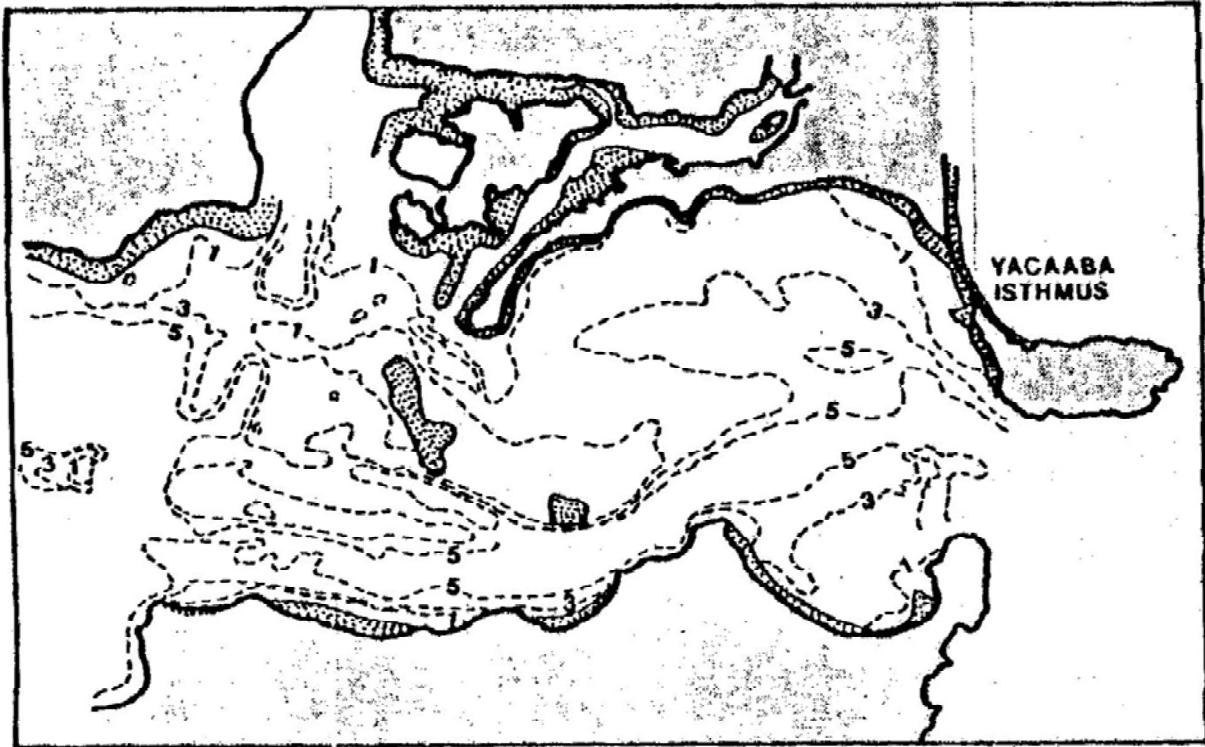


**1828 - WILLIAM JOHNS**

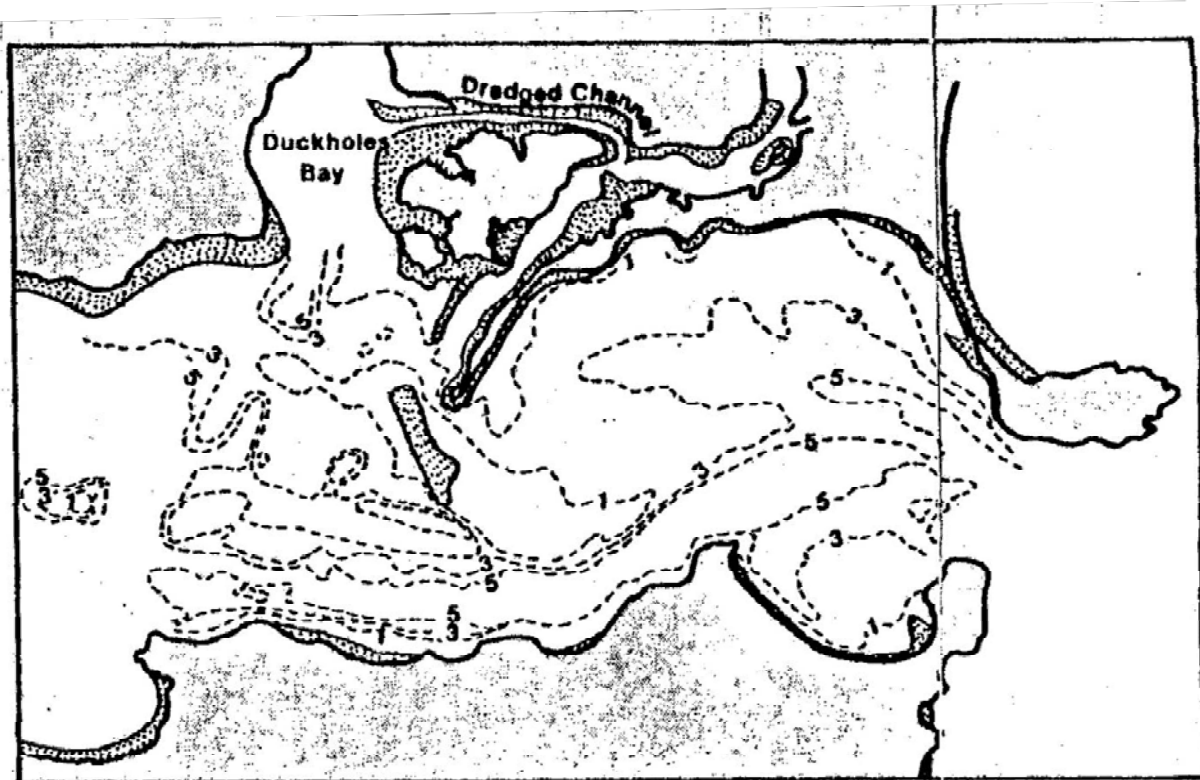


**1838 - JOHNSON**  
( DEPTH IN FATHOMS )





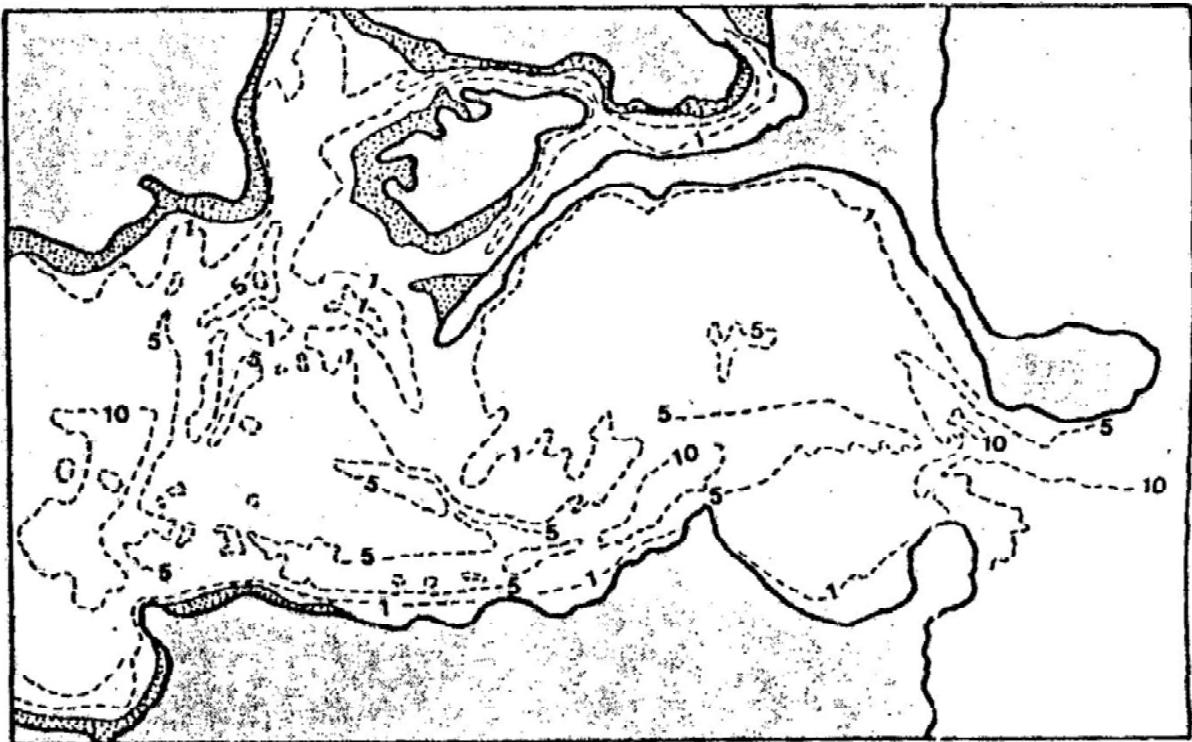
**1866 - F.W. SIDNEY R.N.**  
(DEPTH IN FATHOMS)



**1909 - F.W. SIDNEY**  
(CORRECTIONS BY G.H. HALLIGAN)

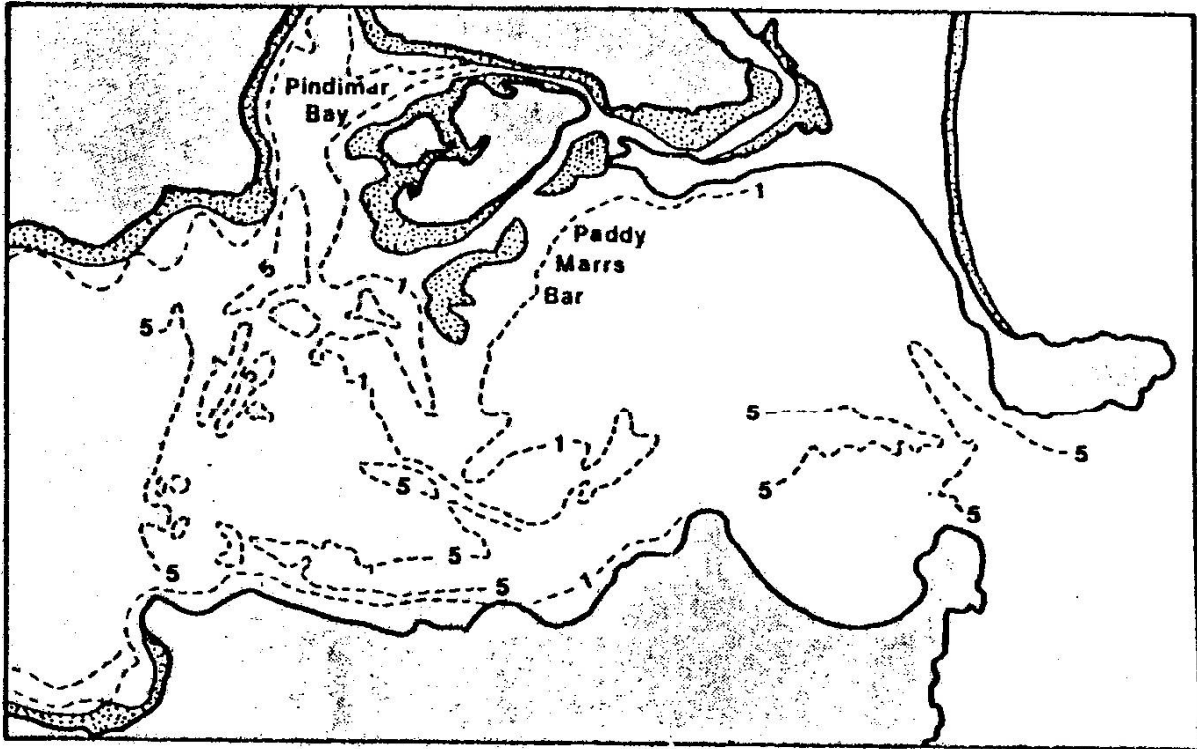


**1920 - C.M.L. SCOTT**  
(DEPTH IN FATHOMS)

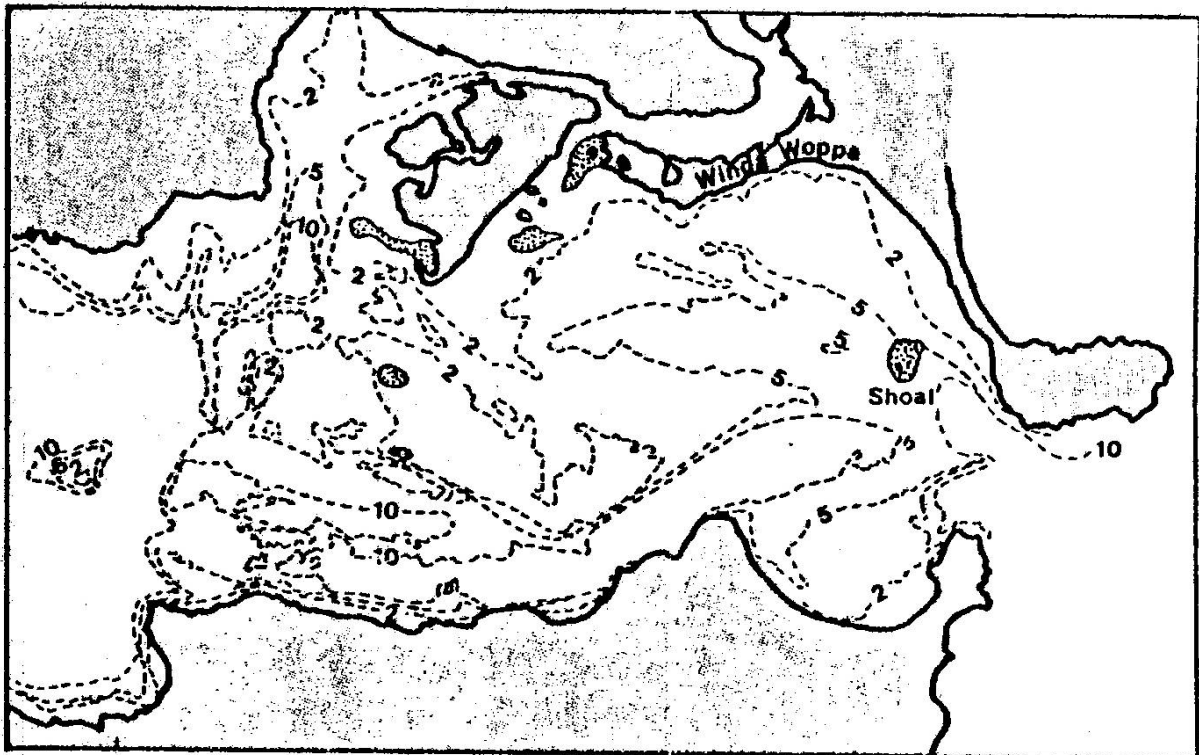


**1922 - SOURCE OF BATHYMETRY UNKNOWN**  
(DEPTH IN FATHOMS)





**1941 - SOURCE OF BATHYMETRY UNKNOWN**  
( DEPTH IN FATHOMS )



**1969 - P.W.D. SURVEY**  
( DEPTH IN METRES )

## APPENDIX B: WIND AND WAVE DATA

Table B-1 Percentage Occurrence Wave Height, Sydney March 1992 to June 2009

H <sub>s</sub> (m)	JAN	FEB	MAR	APR	MAY	JUN	JUL	AUG	SEP	OCT	NOV	DEC	TOTAL
0 – 0.49	100	100	100	100	100	100	100	100	100	100	100	100	100
0.5 – 0.99	99.96	99.99	100	99.9	99.61	99.54	99.71	99.43	99.95	99.84	99.89	99.91	99.803
1 – 1.49	89.44	88.99	91.98	87.62	79.15	77.68	79.34	77.75	79.85	85.05	87.56	84.13	83.784
1.5 – 1.99	47.28	49.75	52.45	49.23	50.31	49.05	46.83	43.07	41.47	45.35	46.61	44.63	47.12
2 – 2.49	18.65	21.05	24.41	25.67	27.42	27.75	26.28	21.73	19.74	18.82	21.45	18.89	22.777
2.5 – 2.99	6.43	8.3	10.78	11.82	12.65	15.69	14.53	10.29	9.1	8.15	10.54	7.36	10.595
3 – 3.49	2.72	2.94	5.19	6.02	6.48	9.42	7.61	5.47	4.49	4.05	5.69	2.99	5.349
3.5 – 3.99	1.03	1.22	2.71	3.14	2.67	5.72	3.96	2.63	1.88	2.15	3.22	1.18	2.676
4 – 4.49	0.3	0.51	1.04	1.52	1.16	3.45	2.32	1.56	0.86	1.16	1.59	0.44	1.361
4.5 – 4.99	0.07	0.22	0.53	0.67	0.7	1.97	1.38	0.81	0.47	0.43	0.89	0.16	0.714
5 – 5.49	0	0.05	0.33	0.25	0.59	1.13	0.62	0.37	0.08	0.12	0.42	0.04	0.345
5.5 – 5.99	0	0.01	0.2	0.08	0.37	0.68	0.3	0.13	0.03	0.06	0.18	0	0.177
6 – 6.49	0	0	0.08	0.03	0.19	0.27	0.18	0.02	0	0	0.03	0	0.071
6.5 – 6.99	0	0	0.01	0	0.15	0.03	0.07	0	0	0	0	0	0.023
7 – 7.49	0	0	0	0	0.11	0	0	0	0	0	0	0	0.01
7.5 – 7.99	0	0	0	0	0.05	0	0	0	0	0	0	0	0.004
8 – 8.49	0	0	0	0	0.04	0	0	0	0	0	0	0	0.003
8.5 – 8.99	0	0	0	0	0	0	0	0	0	0	0	0	0
<b>Average (m) :</b>	1.57	1.62	1.79	1.63	1.67	1.73	1.66	1.55	1.54	1.58	1.61	1.54	1.63
<b>Maximum (m) :</b>	4.92	5.53	6.61	6.18	8.43	6.87	6.96	6.09	5.78	5.81	6.22	5.49	8.43
<b>Minimum (m):</b>	0.48	0.5	0.59	0.38	0.4	0.39	0.39	0.4	0.45	0.43	0.38	0.46	0.38

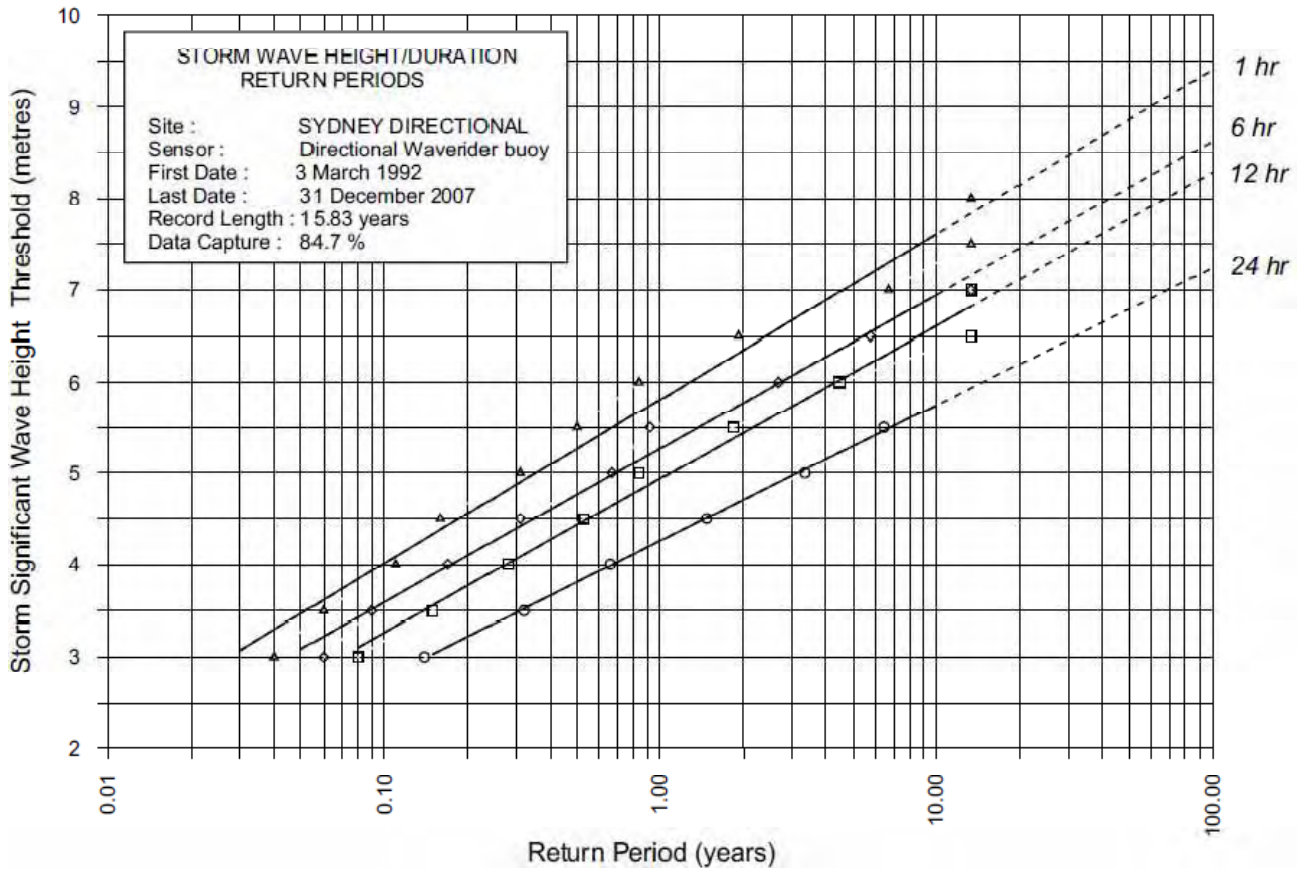


Figure B-1 Wave Height / Duration Curves for Sydney (MHL, 2009)

Table B-2 Percentage Occurrence Wave Direction, Sydney, March 1992 – June 2009

DIR	DEGREES	JAN	FEB	MAR	APR	MAY	JUN	JUL	AUG	SEP	OCT	NOV	DEC	TOTAL
N	348.75 - 11.24	0	0	0	0	0	0	0	0	0	0	0	0	0
NNE	11.25 - 33.74	0.16	0.01	0.06	0.1	0.06	0.05	0.04	0.11	0.09	0.26	0.04	0.09	0.091
NE	33.75 - 56.24	4.4	2.87	2.66	2.06	1.37	1.07	0.87	1.63	4.94	5.83	4.4	5.15	3.057
ENE	56.25 - 78.74	16.62	14.07	9.77	6.51	6.33	3.54	3.5	4.7	9.85	11.1 9	13.77	11.7 2	9.033
E	78.75 - 101.24	18.83	17.68	16.74	11.5 6	9.67	8.6	9.48	5.64	7.66	9.3	9.85	10.5 6	11.086
ESE	101.25 - 123.74	11.05	13.32	12.73	13.6 8	10.25	9.98	12.51	7.46	6.77	7.63	8.66	9.11	10.227
SE	123.75 - 146.24	11.98	12.16	17.1	18.8 6	18.22	17.03	19.38	20.21	17.32	13.0 8	14.18	14.3 6	16.312
SSE	146.25 - 168.74	18.82	20.18	24.59	30.0 3	34.13	40.23	35.74	39.73	32.94	29.3 5	24.22	24.9 3	29.998
S	168.75 - 191.24	16.9	19.07	15.26	16.4 1	18.91	18.7	16.59	19.09	18.81	21.6 7	23.02	22.5 9	18.884
SS W	191.25 - 213.74	1.22	0.65	1.06	0.64	0.52	0.41	0.76	0.84	0.85	1.41	1.82	1.39	0.954
SW	213.75 - 236.24	0	0	0.03	0.1	0.11	0.05	0.22	0.03	0.15	0.07	0	0.02	0.067
WS W	236.25 - 258.74	0	0	0	0	0.03	0.03	0.1	0.05	0.16	0.05	0.03	0.01	0.04
W	258.75 - 281.24	0.01	0	0	0.04	0.05	0.12	0.27	0.12	0.15	0.05	0.01	0.02	0.073
WN W	281.25 - 303.74	0	0	0	0	0.1	0.07	0.28	0.1	0.17	0.1	0.01	0.03	0.077
NW	303.75 - 326.24	0	0	0	0	0.16	0.08	0.15	0.19	0.08	0.02	0	0.02	0.062
NN W	326.25 - 348.74	0	0	0	0	0.06	0.03	0.08	0.08	0.01	0	0	0.01	0.024
	Average :	120.3 7	123.6	128.1 2	135. 53	138.7 9	144.56	142.6 9	144.96	136.6 4	134. 06	132.3	133. 07	134.87
	Maximum :	277	208	221	281	351	357	358	355	356	325	297	330	358
	Minimum :	21	33	21	3	20	10	23	15	0	20	33	7	0



**Table B-3 Percentage Occurrence Wave Period, Sydney March 1992 to June 2009**

T <sub>p</sub> (s)	JAN	FEB	MAR	APR	MAY	JUN	JUL	AUG	SEP	OCT	NOV	DEC	TOTAL
0.00 - 1.99	0	0	0	0	0	0	0	0	0	0	0	0	0
2.00 - 3.99	0.08	0.05	0.06	0.17	0.46	0.51	0.72	0.66	0.59	0.35	0.14	0.27	0.353
4.00 - 5.99	8.56	7.44	4.03	5.38	3.13	2.34	3.2	4.21	6.05	9.1	9.59	9.88	5.962
6.00 - 7.99	27.13	23.32	13.87	10.85	8.37	8.43	6.37	10.75	15.04	20.56	25.38	25.23	15.848
8.00 - 9.99	31.15	28.89	30.23	26.01	26.74	21.43	22.33	22.32	27.76	26.59	29.9	26.91	26.513
10.00 - 11.99	26.1	25.68	32.01	34.01	38.84	37.5	41.89	37.33	33.76	29.16	27.3	26.91	32.884
12.00 - 13.99	6.13	12.71	16.82	19.13	17.68	23.36	20.06	18.92	12.53	10.28	7.08	9.48	14.759
14.00 - 15.99	0.71	1.72	2.72	3.64	3.96	5.31	4.84	4.7	3.5	2.76	0.61	1.24	3.067
16.00 - 17.99	0.14	0.19	0.24	0.7	0.74	1.09	0.54	1.08	0.68	1.01	0.01	0.06	0.56
18.00 - 19.99	0	0	0.02	0.09	0.07	0.04	0.05	0.03	0.11	0.14	0	0.02	0.049
20.00 - 21.99	0	0	0	0.02	0	0	0	0	0	0.05	0	0	0.006
<b>Average (s) :</b>	<b>8.81</b>	<b>9.29</b>	<b>10.03</b>	<b>10.28</b>	<b>10.32</b>	<b>10.81</b>	<b>10.56</b>	<b>10.33</b>	<b>9.77</b>	<b>9.38</b>	<b>8.88</b>	<b>9.04</b>	<b>9.78</b>
<b>Maximum (s) :</b>	<b>17.1</b>	<b>17.1</b>	<b>19.7</b>	<b>20</b>	<b>19.7</b>	<b>19.7</b>	<b>18.18</b>	<b>18.18</b>	<b>19.7</b>	<b>20</b>	<b>17.1</b>	<b>19.7</b>	<b>20</b>
<b>Minimum (s):</b>	<b>3.33</b>	<b>3.8</b>	<b>3</b>	<b>2.8</b>	<b>2.77</b>	<b>2.8</b>	<b>2.85</b>	<b>2.77</b>	<b>3</b>	<b>2.6</b>	<b>3.4</b>	<b>2.6</b>	<b>2.6</b>

**Table B-4 Maximum Yearly Wind Speeds for Wind Direction Octants (Williamstown)**

Year	NN	NE	EE	SE	SS	SW	WW	NW
1989	31	39	48	46	48	55	50	55
1990	26	44	48	52	59	46	63	65
1991	30	44	46	42	50	48	67	65
1992	33	42	44	50	54	52	65	61
1993	41	37	39	46	50	48	63	63
1994	37	46	44	57	57	41	70	65
1995	37	39	41	48	55	54	57	55
1996	35	44	37	55	55	37	55	59
1997	28	39	48	39	55	44	55	46
1998	22	35	33	44	48	52	63	74
1999	18	33	35	42	46	59	59	57
2000	26	37	39	44	46	41	59	50
2001	30	39	41	48	57	41	50	61
2002	24	37	42	39	44	41	50	59
2003	35	39	39	41	50	46	57	72
2004	35	35	37	44	46	48	57	63
2005	28	33	39	46	54	52	65	54
2006	28	35	52	52	50	52	52	44
2007	28	33	39	67	42	37	57	55
2008	28	31	37	44	48	52	59	57
2009	33	33	41	46	50	39	63	65
<b>MAX</b>	<b>41</b>	<b>46</b>	<b>52</b>	<b>67</b>	<b>59</b>	<b>59</b>	<b>70</b>	<b>74</b>

## APPENDIX C: SCENARIO SELECTION FOR MORPHOLOGICAL MODELLING

To assess the impacts of dredging options on the morphology of the Eastern Channel and Myall Spit data were required that would generate a reasonable sediment transport. Historical aerial photographs were examined to identify periods when the Eastern Channel experienced significant infilling Myall Spit grew notably.

- The Spit extended significantly between 2001 and 2009;
- A review of SPOT imagery for years 2005 and 2007 showed that a navigable channel was still present in February 2005 although the western extent of the spit was beginning to encroach on the eastern side of the channel;
- Aerial photos (DECCW) from April 2006 show that the east side (i.e. east of the pile of rock 'ballast' in the centre of the channel) of the channel was blocked by westward migration of the spit at that time.

Based on the timing of these features we examined wave data between February 2005 and April 2006.

The data revealed that notable swell wave events occurred between March-April 2005 and June-July 2005. The south east facing alignment of shorelines within the study region is most vulnerable to swell waves originating from the south-east (SE). The March-April event had the more significant south-easterly waves and that event was subsequently chosen for analyses. This event was not responsible for all of the spit extension and channel infilling present between February, 2005 and April, 2006, but would have contributed a significant proportion. The time series of ocean wave heights and identification of those originating from the south east is shown on Figure D-1.

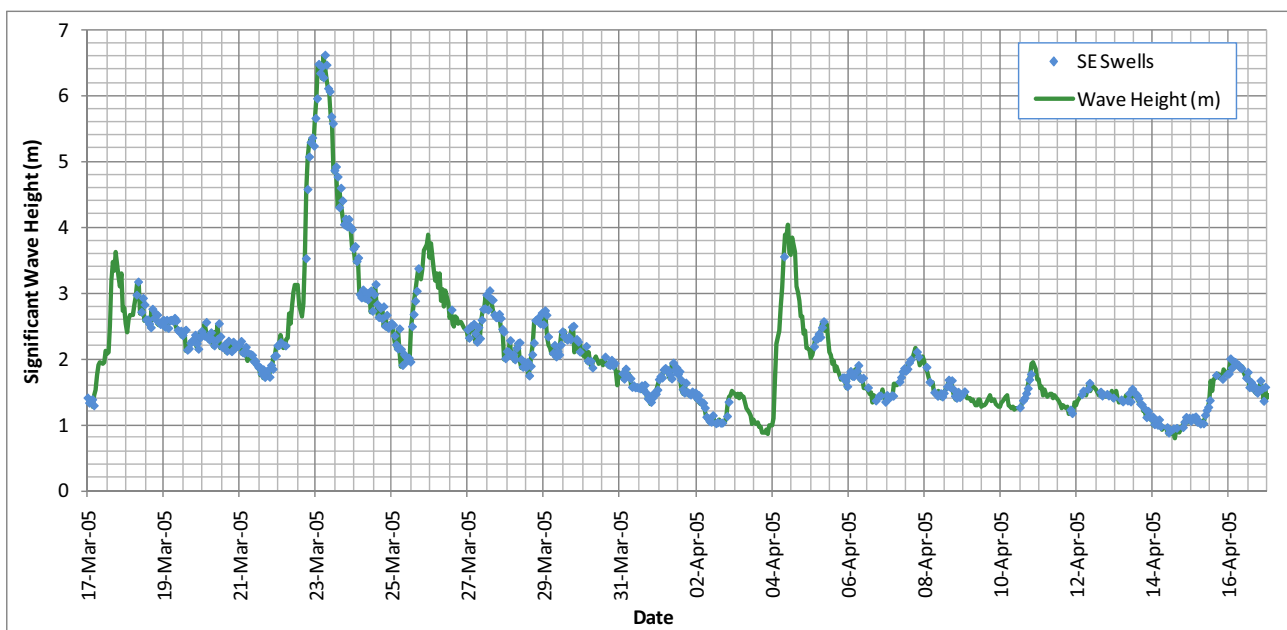


Figure C-1 Wave Climate for Sydney from 17<sup>th</sup> March to 17<sup>th</sup> April 2005

## APPENDIX D: LONGSHORE SEDIMENT TRANSPORT CALCULATIONS

### D.1 Types of Waves

Longshore sediment transport rates were calculated separately for the following two different types of waves impacting on Winda Woppa:

- Local wind waves caused by winds blowing over the surface of Port Stephens; and
- Ocean Swell waves propagating in through the entrance of Port Stephens.

### D.2 Transects used for Calculation

Longshore Transport rates were calculated at three transects established along Winda Woppa spit, as shown on Figure D.2. For longshore transport calculations, it is necessary to examine the characteristics of breaking waves. SWAN was used to determine breaking wave directions and heights along these transects for numerous local wind wave and ocean swell wave conditions.

### D.3 Wind Speed Statistics and Local Wind Wave Simulations

Wind statistics were derived from the 20 year wind record collected at Williamtown, and data organised into 45 degree bins. The proportion of time wind occurred from each direction is charted on Figure D.1.

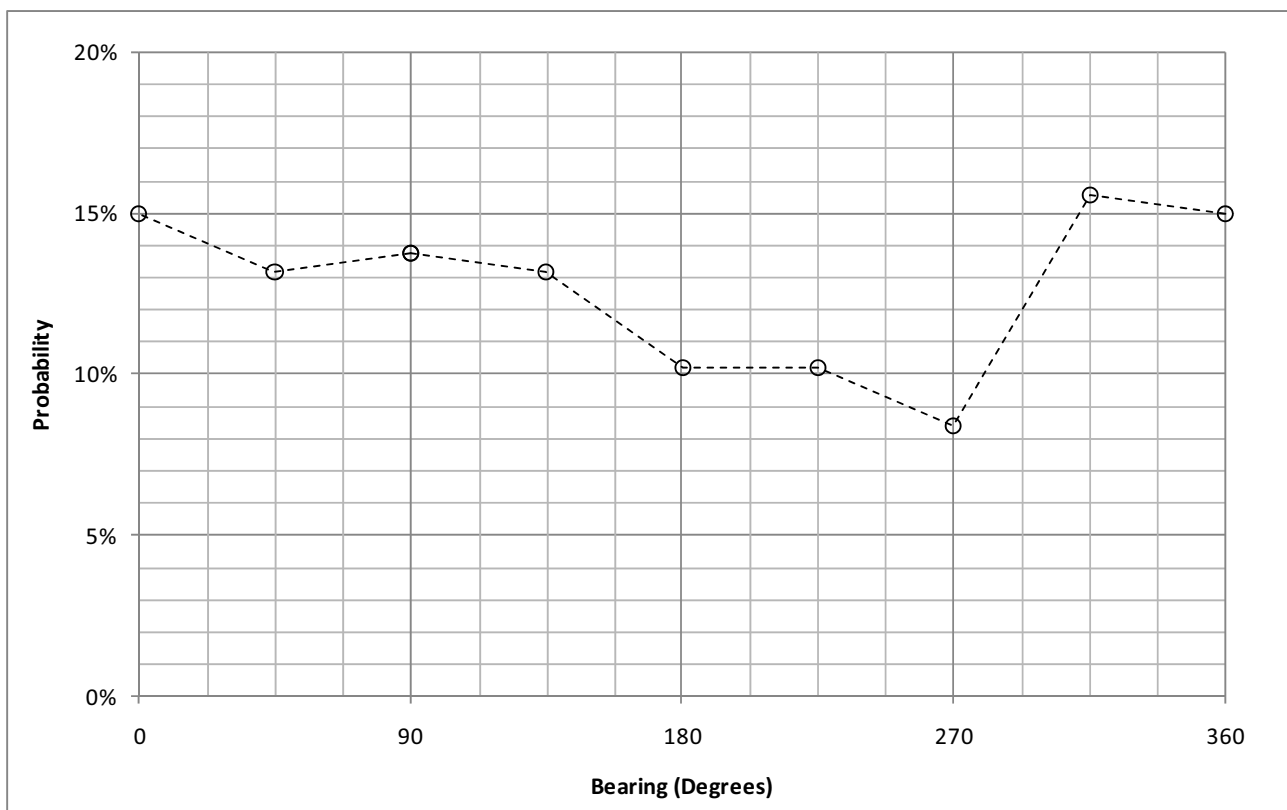








Figure D-1 Prevalence of Winds from each direction





**Legend**

-  Dredging Location
-  Erosion location
-  Transects
-  Predominant swell direction
-  Swell driven longshore transport
-  Wind driven longshore transport

Title: **Dredging option through deposition near Winda Woppa**

Figure: **D-2**

Rev: **A**

BMT WBM endeavours to ensure that the information provided in this map is correct at the time of publication. BMT WBM does not warrant, guarantee or make representations regarding the currency and accuracy of information contained in this map.



The data in each directional bin were subsequently subdivided into bins based on ranges in wind speed of  $2 \text{ km}\cdot\text{h}^{-1}$ . Wind data from each directional bin was ranked in order of probability based on the statistical analysis previously undertaken. All bins with a probability greater than 0.3 percent were considered as separate scenarios. All other cases were considered to be statistically insignificant.

A SWAN wave model simulation was executed for each case, using a direction and wind speed from the representative bins. The height and direction of the resultant breaking waves was determined and used in the longshore transport calculation.

The resulting longshore transport rates are assumed to occur for the same proportion of time as the corresponding wind condition when deriving annualised (average) longshore transport rates.

### D.4 Ocean Swell Statistics and Swell Propagation Simulations

Ocean swell statistics were derived by analysing the WaveRider data from Sydney over a period of 15 years. Data were organised into 22.5 degree bins. Swell occurred between bearings of 45 and 225 degrees (NW to SE) due to the orientation of the coastline. The proportion of time swell occurs from each direction is charted on Figure D.3.

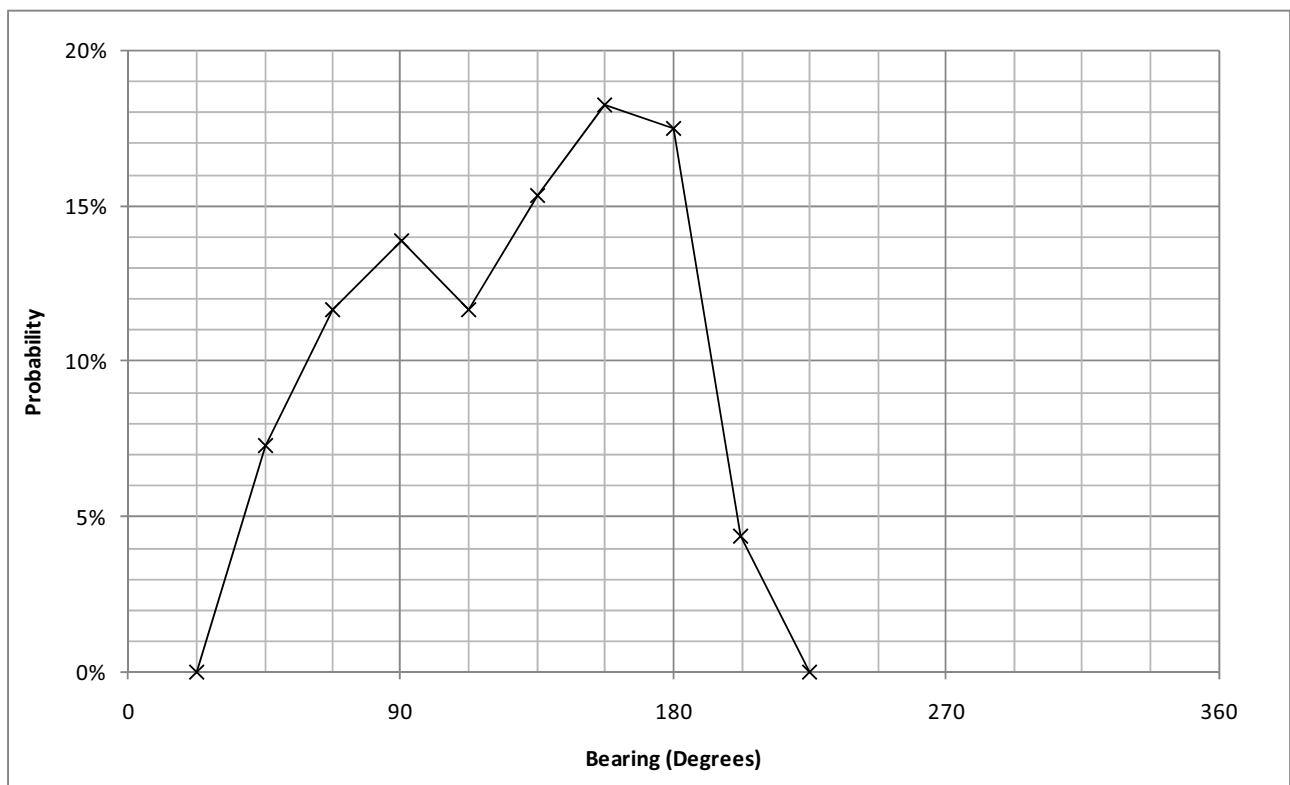


**Figure D-3 Prevalence of Ocean Swell from each direction**

The data in each directional bin was further subdivided into bins based on the wave period which ranged between 4.5 and 17 seconds. Each of the direction/wind speed bins was assigned a probability based on the proportion of time winds fell within that bin in the wave record. Bins with a probability of less than 0.01 percent were considered to be statistically insignificant.



Probability distributions of swell wave heights for each of these bins were obtained through statistical analysis. Wave height cases were defined for each bin representing an exceedance probability of 20, 40, 60 and 80 percent.

A SWAN wave model simulation was subsequently executed for each case, using a direction, period and wave height representative of that case. The height and direction of the resultant breaking wave was determined and used in the longshore transport calculation.

The resulting longshore transport rates are assumed to occur for the same proportion of time as the corresponding wind condition when deriving annualised (average) longshore transport rates.

## D.5 Longshore Transport Calculations

Sediment transport in water can be represented in terms of scouring and advection dispersion processes. In the surf zone both current and wave action significantly alter the scouring and transport processes. The calculation of Longshore Transport Rates is relatively inaccurate. Therefore, three different methods for calculating the longshore transport were used for comparison and consideration in deriving a representative number.

The CERC, Kamphuis and Van Rijn LT Formulas have been used to calculate approximations of longshore sediment transport based on the statistically weighted wind wave and swell conditions described in preceding sections. Longshore sediment transport is greatest when waves approach the shore at an angle of 45 degrees.

While small in magnitude, tidal current velocities are also important, particularly as the tidal hydrodynamics tend to drive currents from east to west for the majority of the tidal cycle. During the flood tide, the TUFLOW-FV model indicates that sand is dragged towards the eastern channel under the effect of the prevailing current. However, during the ebb current, TUFLOW-FV indicates a counter clockwise eddy forms between the main ebb jet of the tide and the shoreline along Winda Woppa. This causes currents adjacent to the shoreline to be from east to west during most of the ebb tide as well.

The CERC Formula is commonly applicable to high energy storm conditions, in which it over predicts by an order of magnitude of approximately two. However, the degree of over prediction is significantly higher for standard wave conditions (as applied for this assessment). The CERC Formula has been used in this instance as a benchmark, as it has a longer track record of application for longshore sediment transport calculation.

The Kamphuis equation has generally been considered an underestimate of longshore sediment transport; however for low wave breaking wave heights it can also over estimate rates. The Kamphuis method always calculated lower transport rates than with Van Rijn's equation in this assessment.

The van Rijn LT formulation has an advantage over the other formulations in that the tidal current (as opposed to the current generated by waves) is an input to the calculation.

## D.6 Longshore Transport Due to Swell - Results

The resulting breakdown of swell related annualised sediment transport rates at Transect 1 plotted against offshore swell direction is presented on Figure D.4. Transect 1 has been presented, as



results at this transect best represent the measured deposition in the eastern channel over the past 10 years.

Transport is maximised for swell bearings between 90 and 135 degrees (i.e. swell arriving from the east through to south). At this approach angle, swell waves have a more direct line of attack to the foreshore at Winda Woppa.

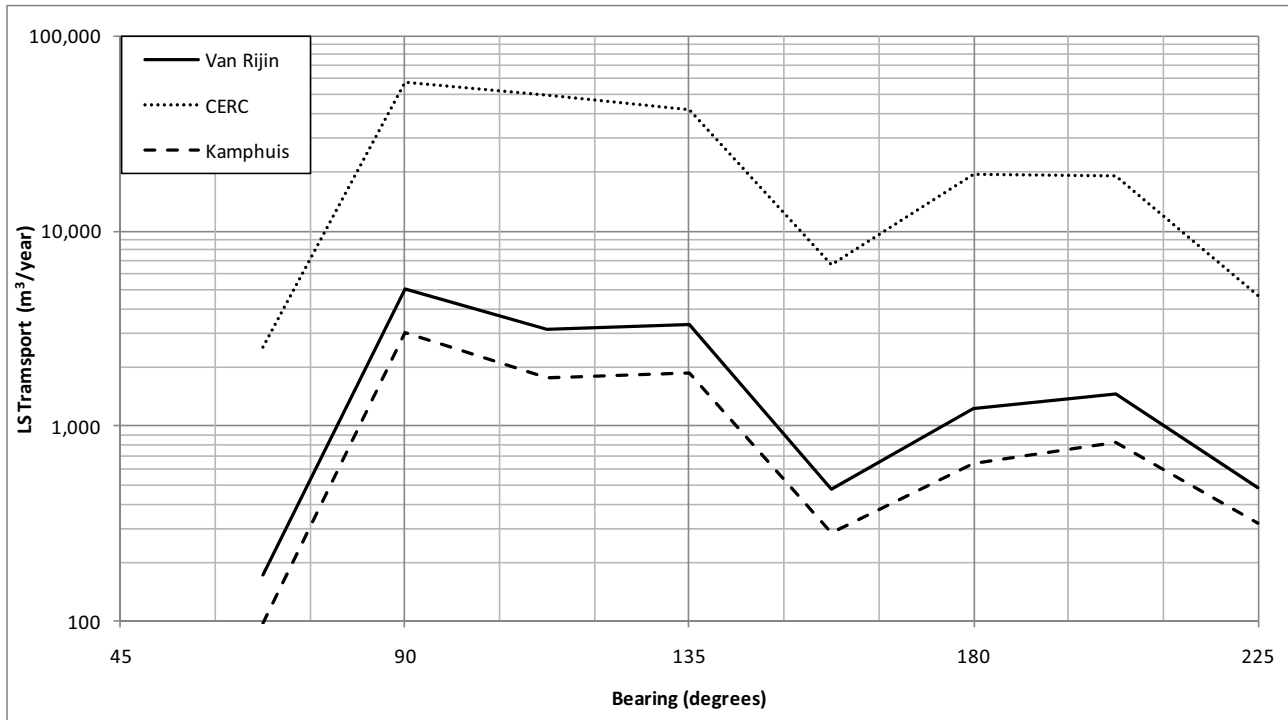


**Figure D-4 Relative Rates of Longshore Sediment Transport Volumes Expected for Specific Offshore Swell Directions**

### D.7 Longshore Transport Due to Wind - Results

Longshore transport rates are the greatest for winds approaching from between 90 and 180 degrees (E to S winds). This is because the direction of the wind generated waves are oblique to the shoreline in at Winda Woppa. For wind bearings greater than 180 degrees transport is either negative (indicating transport away from the river mouth) or very low as it tends to push sand towards the east. However, the overall annualised magnitude of transport due to wind waves remains positive. Overall, wind wave induced longshore transport at this location is around an order of magnitude less than that caused by ocean swell.

### D.8 Net Transport and Comparison to Hydrosurvey Data

The total transport rate was considered to result from both wind and swell generated waves. A summary of net long shore transport rates, from both Swell and wind waves are presented in Table D-1. These values are an average of the Kamphuis and Van Rijn computations. Figure D-2 schematically illustrates the LS sediment transport occurring at each transect.

**Table D-1 Contributors to Net Annualised Longshore Transport Rate**

Transect	Annualised Swell Related Transport	Annualised Wind Wave Related Transport	Annualised 'Total' Transport
1	12 100	250	12 350
2	2 000	40	2 040
3	1 300	90	1 390

+ve Transport rates indicate transport from east to west (i.e. towards the eastern channel)

Tables D-2 to D-19, at the end of this Appendix show this data further broken down for each computation method. These Tables help illustrate the variation in transport that occurs along this shore, due to the variable orientation to incoming waves.

By comparing the differences in volume between the 2009 and 2001 hydrosurveys, it is clear that around 100 000 m<sup>3</sup> of sand has deposited at the end of Winda Woppa Spit. This is consistent with an annualised total transport of around 12 000 m<sup>3</sup>/yr, consistent with the eastern most transect (Transect 1). The fit between the measured and modelled results is remarkable, given the uncertainties associated with longshore transport calculations. In interpreting this information, it should be noted that there are errors inherent in both the longshore transport calculations, and the comparison of hydrosurvey data. Transport in the area is complex and the ultimate fate of sand transported along Winda Woppa may be dictated by tides, wind and other factors.

## D.9 Where did the sand come from?

From examination of aerial photography, it is clear that the shoreline to the west of Barnes Rock has receded significantly over the past decade.

Again, using the digital elevation models available, the volume represented by that recession has been estimated. This is somewhat difficult, as we do not have ground survey data for the dunes in this area from 2001.

Based on Lidar data, we note that the dunes in this area have crest levels of around 3.0 m. Comparing the bathymetries of 2001 and 2009, we note that the relatively inactive bed level (i.e. minimal change between 2001 and 2009) is at around -1.0 m AHD.

Considering a number of transects across the area of recession, we have determined that the linear amount of recession (based on location of the front edge of any visible foredune vegetation from aerial photographs) as measured in GIS averages around 70 m. This occurs over around 300 m of foreshore.

The length of foreshore subject to recession is around 300 m. Assuming similar dune and beach profiles existed in 2001, our estimate is based on a 4.0 m high dune receding by 70 m. This results in a volume of sand loss of around 84,000 m<sup>3</sup>.

The calculated eroded volume is similar to that calculated as depositing at the end of Winda Woppa from the comparison of hydrosurveys. However, the available data is limited, and it is possible that the estimates could vary by +/- 30%

Nevertheless, it is fair to conclude, on the basis of this calculation, and the apparent relative stability of shorelines immediately to the north of Barnes Rock (i.e. south of the main area of erosion) that the sand removed from this area by wave action supplied most of the sediment needed to grow Winda Woppa spit.

It follows that the amount of sediment transported around Barnes Rock (i.e. from Jimmy's Beach) is not likely to be a significant factor in causing the elongation of Winda Woppa spit.



D.10 Longshore Computation Tables

D.10.1 Transect 1

**Swell waves**

**Table D-2: Swell generated annual longshore transport rates at Transect 1 calculated using the Kamphuis Method**

KAMPHUIS		Bearing (degrees)								
		45	62.5	90	112.5	135	157.5	180	202.5	Total
		Longshore Transport rates (m <sup>3</sup> /year)								
Period (sec)	<6	19	78	4	5	64	93	103	11	378
	6-8	78	555	380	6	8	27	517	294	1,864
	8-10	0	1,159	671	193	45	105	167	10	2,350
	10-12	0	1,110	563	1,445	71	408	28	0	3,625
	12-14	0	99	49	221	93	7	0	0	470
	>14	0	0	118	10	0	0	0	0	128
	Total	97	3,001	1,785	1,879	281	640	816	316	8,816

**Table D-3: Swell generated annual longshore transport rates at Transect 1 calculated using the CERC Method**

CERC		Bearing (degrees)								
		45	62.5	90	112.5	135	157.5	180	202.5	Total
		Longshore Transport rates (m <sup>3</sup> /year)								
Period (sec)	<6	999	2,528	110	104	735	1,657	1,652	236	8,022
	6-8	1,536	11,107	5,500	340	301	1,378	11,742	4,265	36,168
	8-10	0	22,578	14,770	4,348	1,780	2,773	5,239	150	51,639
	10-12	0	17,791	24,411	32,297	2,313	13,373	544	0	90,729
	12-14	0	3,292	2,020	4,107	1,554	374	9	0	11,356
	>14	0	7	2,472	203	0	7	0	0	2,689
	Total	2,535	57,303	49,283	41,399	6,684	19,563	19,186	4,650	200,603

**Table D-4: Swell generated annual longshore transport rates at Transect 1 calculated using the Van Rijn Method**

Van Rijn		Bearing (degrees)								
		45	62.5	90	112.5	135	157.5	180	202.5	Total
		Longshore Transport rates (m <sup>3</sup> /year)								
Period (sec)	<6	46	150	7	7	93	148	153	18	621
	6-8	128	969	585	12	14	58	940	455	3,161
	8-10	0	1,981	1,115	313	86	184	332	14	4,025
	10-12	0	1,774	1,187	2,623	132	833	44	0	6,594
	12-14	0	192	97	372	148	16	0	0	825
	>14	0	36	197	22	0	0	0	0	255
	Total	173	5,102	3,187	3,349	473	1,239	1,470	488	15,480

**Wind waves**

**Table D-5: Wind generated annual longshore transport rates at Transect 1 calculated using the Kamphuis Method**

Kamphuis		Direction (Bearing)								
		0	45	90	135	180	225	270	315	Total
<b>Longshore Transport rates (m<sup>3</sup>/year)</b>										
Speed (m·s <sup>-1</sup> )	0-4	0.00	0.00	0.21	0.42	-0.18	-1.39	-0.11	0.00	<b>-1.04</b>
	4-8	0.00	0.06	8.36	26.29	7.97	-8.05	-0.71	0.00	<b>33.92</b>
	8-12	0.00	0.10	8.19	32.35	18.10	-6.19	-1.00	0.00	<b>51.54</b>
	12-16	0.00	0.00	0.00	4.74	4.67	-0.77	-0.38	0.00	<b>8.26</b>
	Total	<b>0.00</b>	<b>0.16</b>	<b>16.75</b>	<b>63.80</b>	<b>30.56</b>	<b>-16.40</b>	<b>-2.19</b>	<b>0.00</b>	<b>92.68</b>

**Table D-6: Wind generated annual longshore transport rates at Transect 1 calculated using the CERC Method**

CERC		Direction (Bearing)								
		0	45	90	135	180	225	270	315	Total
<b>Longshore Transport rates (m<sup>3</sup>/year)</b>										
Speed (m·s <sup>-1</sup> )	0-4	0.00	10.88	183.64	327.31	116.39	-110.62	-7.27	0.00	<b>520.32</b>
	4-8	-0.01	72.50	2260.22	5708.47	3576.89	-540.22	-43.56	0.00	<b>11034.29</b>
	8-12	0.00	56.49	1592.50	4725.18	5360.66	-340.76	-55.77	0.00	<b>11338.29</b>
	12-16	0.00	0.00	0.00	471.08	943.89	-33.90	-19.00	-0.01	<b>1362.06</b>
	Total	<b>-0.01</b>	<b>139.88</b>	<b>4036.36</b>	<b>11232.04</b>	<b>9997.83</b>	<b>-1025.50</b>	<b>-125.61</b>	<b>-0.01</b>	<b>24254.97</b>

**Table D-7: Wind generated annual longshore transport rates at Transect 1 calculated using the Van Rijn Method**

Van Rijn		Direction (Bearing)								
		0	45	90	135	180	225	270	315	Total
<b>Longshore Transport rates (m<sup>3</sup>/year)</b>										
Speed (m·s <sup>-1</sup> )	0-4	0.00	0.03	1.01	2.07	0.71	-0.28	-0.01	0.00	<b>3.52</b>
	4-8	0.00	0.31	30.14	91.01	34.62	-2.52	-0.09	0.00	<b>153.46</b>
	8-12	0.00	0.39	27.60	103.20	71.44	-2.18	-0.17	0.00	<b>200.29</b>
	12-16	0.00	0.00	0.00	14.04	16.96	-0.30	-0.08	0.00	<b>30.61</b>
	Total	<b>0.00</b>	<b>0.72</b>	<b>58.75</b>	<b>210.31</b>	<b>123.73</b>	<b>-5.28</b>	<b>-0.34</b>	<b>0.00</b>	<b>387.88</b>

D.10.2 Transect 2

**Swell waves**

**Table D-8: Swell generated annual longshore transport rates at Transect 2 calculated using the Kamphuis Method**

KAMPHUIS		Bearing (degrees)								
		45	62.5	90	112.5	135	157.5	180	202.5	Total
		Longshore Transport rates (m <sup>3</sup> /year)								
Period (sec)	<6	5	17	1	1	11	17	21	2	75
	6-8	15	99	62	1	1	4	98	53	333
	8-10	0	206	157	43	7	16	34	2	466
	10-12	0	200	108	273	12	84	4	0	682
	12-14	0	22	9	39	17	1	0	0	88
	>14	0	0	21	2	0	0	0	0	23
	Total	20	545	359	358	48	123	157	57	1,667

**Table D-9: Swell generated annual longshore transport rates at Transect 2 calculated using the CERC Method**

CERC		Bearing (degrees)								
		45	62.5	90	112.5	135	157.5	180	202.5	Total
		Longshore Transport rates (m <sup>3</sup> /year)								
Period (sec)	<6	305	632	25	16	138	406	351	39	1,912
	6-8	401	2,148	971	45	47	254	2,407	848	7,120
	8-10	0	4,442	3,673	1,058	308	499	1,209	25	11,215
	10-12	0	3,518	4,743	6,726	476	3,094	91	0	18,648
	12-14	0	833	433	783	305	73	1	0	2,428
	>14	0	2	469	37	0	2	0	0	509
	Total	706	11,575	10,315	8,666	1,274	4,328	4,058	912	41,833

**Table D-10: Swell generated annual longshore transport rates at Transect 2 calculated using the Van Rijn Method**

Van Rijn		Bearing (degrees)								
		45	62.5	90	112.5	135	157.5	180	202.5	Total
		Longshore Transport rates (m <sup>3</sup> /year)								
Period (sec)	<6	11	27	1	1	13	24	25	2	104
	6-8	22	139	77	1	1	8	143	66	456
	8-10	0	284	209	56	11	23	57	2	642
	10-12	0	257	177	404	19	144	5	0	1,006
	12-14	0	36	15	52	21	2	0	0	126
	>14	0	6	28	3	0	0	0	0	36
	Total	32	749	507	517	65	200	230	70	2,370

**Wind waves****Table D-11: Wind generated annual longshore transport rates at Transect 2 calculated using the Kamphuis Method**

Kamphuis		Direction (Bearing)								
		0	45	90	135	180	225	270	315	Total
<b>Longshore Transport rates (m<sup>3</sup>/year)</b>										
Speed (m·s <sup>-1</sup> )	0-4	0.00	0.00	0.10	0.32	-0.43	-2.01	-0.15	0.00	-2.16
	4-8	0.00	0.01	3.54	13.65	-1.80	-13.30	-1.36	0.00	0.73
	8-12	0.00	0.03	3.44	14.59	-20.32	-11.75	-2.30	0.00	-16.31
	12-16	0.00	0.00	0.00	1.87	-3.72	-1.35	-0.98	0.00	-4.18
	Total	0.00	0.03	7.08	30.43	-26.26	-28.41	-4.80	0.00	-21.92

**Table D-12: Wind generated annual longshore transport rates at Transect 2 calculated using the CERC Method**

CERC		Direction (Bearing)								
		0	45	90	135	180	225	270	315	Total
<b>Longshore Transport rates (m<sup>3</sup>/year)</b>										
Speed (m·s <sup>-1</sup> )	0-4	0.00	1.78	110.84	257.48	32.63	-161.99	-9.99	0.00	230.74
	4-8	0.00	11.43	1113.62	3494.79	1303.41	-964.00	-79.76	0.00	4879.48
	8-12	0.00	13.81	744.01	2610.14	-640.99	-775.09	-132.76	0.00	1819.11
	12-16	0.00	0.00	0.00	194.60	-150.63	-76.77	-54.67	0.00	-87.47
	Total	0.00	27.02	1968.48	6557.00	544.42	-1977.86	-277.19	0.00	6841.87

**Table D-13: Wind generated annual longshore transport rates at Transect 2 calculated using the Van Rijn Method**

Van Rijn		Direction (Bearing)								
		0	45	90	135	180	225	270	315	Total
<b>Longshore Transport rates (m<sup>3</sup>/year)</b>										
Speed (m·s <sup>-1</sup> )	0-4	0.00	0.00	0.45	1.36	0.15	-0.61	-0.02	0.00	1.33
	4-8	0.00	0.03	11.38	42.66	12.56	-6.69	-0.30	0.00	59.64
	8-12	0.00	0.08	10.28	42.81	-5.14	-7.63	-0.70	0.00	39.70
	12-16	0.00	0.00	0.00	4.77	-2.36	-1.05	-0.39	0.00	0.97
	Total	0.00	0.11	22.12	91.60	5.21	-15.99	-1.41	0.00	101.65

D.10.3 Transect 3

**Swell waves**

**Table D-14 Swell generated annual longshore transport rates at Transect 3 calculated using the Kamphuis Method**

KAMPHUIS		Bearing (degrees)								
		45	62.5	90	112.5	135	157.5	180	202.5	ALL
		Longshore Transport rates (m <sup>3</sup> /year)								
Period (sec)	<6	0	0	0	6	0	0	0	0	7
	6-8	0	0	5	46	6	1	1	0	60
	8-10	0	2	55	231	20	3	1	0	312
	10-12	0	5	126	274	25	4	1	0	436
	12-14	0	2	70	80	5	2	0	0	158
	>14	0	2	52	14	0	1	0	0	69
	ALL	0	12	308	652	56	11	4	0	1,042

**Table D-15: Swell generated annual longshore transport rates at Transect 3 calculated using the CERC Method**

CERC		Bearing (degrees)								
		45	62.5	90	112.5	135	157.5	180	202.5	ALL
		Longshore Transport rates (m <sup>3</sup> /year)								
Period (sec)	<6	1	5	17	486	36	18	31	1	595
	6-8	5	50	382	2,504	422	92	133	4	3,593
	8-10	0	157	2,340	7,892	990	193	95	3	11,670
	10-12	0	202	3,774	7,032	931	189	52	0	12,181
	12-14	0	72	1,627	1,623	126	51	5	0	3,504
	>14	0	45	952	249	0	16	0	0	1,263
	ALL	6	531	9,093	19,786	2,505	559	316	9	32,805

**Table D-16: Swell generated annual longshore transport rates at Transect 3 calculated using the Van Rijn Method**

Van Rijn		Bearing (degrees)								
		45	62.5	90	112.5	135	157.5	180	202.5	ALL
		Longshore Transport rates (m <sup>3</sup> /year)								
Period (sec)	<6	0	0	0	13	1	0	0	0	15
	6-8	0	1	9	87	11	2	2	0	111
	8-10	0	3	83	372	32	4	2	0	497
	10-12	0	6	177	401	37	6	1	0	629
	12-14	0	3	90	108	6	2	0	0	209
	>14	0	2	74	30	0	1	0	0	108
	ALL	0	15	434	1,011	86	15	6	0	1,568



**Wind waves****Table D-17: Wind generated annual longshore transport rates at Transect 3 calculated using the Kamphuis Method**

Kamphuis		Direction (Bearing)								
		0	45	90	135	180	225	270	315	Total
<b>Longshore Transport rates (m<sup>3</sup>/year)</b>										
Speed (m·s <sup>-1</sup> )	0-4	0.00	0.00	0.03	0.18	0.21	0.06	0.00	0.00	<b>0.48</b>
	4-8	0.00	0.00	1.28	4.72	7.51	1.50	0.04	0.00	<b>15.05</b>
	8-12	0.00	0.01	1.38	10.37	16.64	2.77	0.10	0.00	<b>31.25</b>
	12-16	0.00	0.00	0.00	0.87	4.07	0.54	0.07	0.00	<b>5.55</b>
	Total	<b>0.00</b>	<b>0.01</b>	<b>2.68</b>	<b>16.14</b>	<b>28.43</b>	<b>4.86</b>	<b>0.20</b>	<b>0.00</b>	<b>52.33</b>

**Table D-18: Wind generated annual longshore transport rates at Transect 3 calculated using the CERC Method**

CERC		Direction (Bearing)								
		0	45	90	135	180	225	270	315	Total
<b>Longshore Transport rates (m<sup>3</sup>/year)</b>										
Speed (m·s <sup>-1</sup> )	0-4	0.00	-0.04	20.89	126.93	198.27	38.60	1.30	0.00	<b>385.96</b>
	4-8	0.01	2.22	386.08	2247.21	3458.71	571.48	19.39	0.00	<b>6685.09</b>
	8-12	0.01	3.34	320.34	2113.62	5132.71	747.76	39.57	0.00	<b>8357.36</b>
	12-16	0.00	0.00	0.00	162.71	858.06	109.53	24.20	0.01	<b>1154.52</b>
	Total	<b>0.01</b>	<b>5.51</b>	<b>727.32</b>	<b>4650.48</b>	<b>9647.76</b>	<b>1467.38</b>	<b>84.46</b>	<b>0.02</b>	<b>16582.93</b>

**Table D-19: Wind generated annual longshore transport rates at Transect 3 calculated using the Van Rijn Method**

Van Rijn		Direction (Bearing)								
		0	45	90	135	180	225	270	315	Total
<b>Longshore Transport rates (m<sup>3</sup>/year)</b>										
Speed (m·s <sup>-1</sup> )	0-4	0.00	0.00	0.04	0.56	0.79	0.05	0.00	0.00	<b>1.44</b>
	4-8	0.00	0.00	2.95	15.58	27.13	3.17	0.02	0.00	<b>48.85</b>
	8-12	0.00	0.02	3.29	29.30	56.56	6.88	0.10	0.00	<b>96.15</b>
	12-16	0.00	0.00	0.00	2.58	12.99	1.38	0.12	0.00	<b>17.07</b>
	Total	<b>0.00</b>	<b>0.02</b>	<b>6.29</b>	<b>48.01</b>	<b>97.46</b>	<b>11.48</b>	<b>0.24</b>	<b>0.00</b>	<b>163.51</b>

# APPENDIX E: MODELLING SOFTWARE AND MODEL ESTABLISHMENT

## E.1 Model Selection

Development of the coastal hydrodynamic model requires a considerable amount of data to adequately represent hydrodynamic, advection / dispersion, waves and sediment transport processes occurring within the study area. The numerical model therefore requires the following datasets to simulate and / or calibrate hydrodynamics:

- **Bathymetric survey data** – used to describe the topography of the bed and coastline over the domain of a numerical model incorporating the full tidal extents of the estuary;
- **Wave, Water level and flow data** – used to calibrate and / or validate model predictions. Wave, Water level and flow data are most commonly used to ensure the model adequately represents the tidal prism of a waterway; and

For the present study, the two-dimensional hydrodynamic model (TUFLOW-FV), coastal wave model (SWAN) and sediment morphology model (TUFLOW-MORPH) were selected to satisfy the modelling scope and objectives. An overview of the selected models is provided in Figure E.1, with further details of model bathymetry, model geometry and boundary condition data adopted for each provided in the following sections.

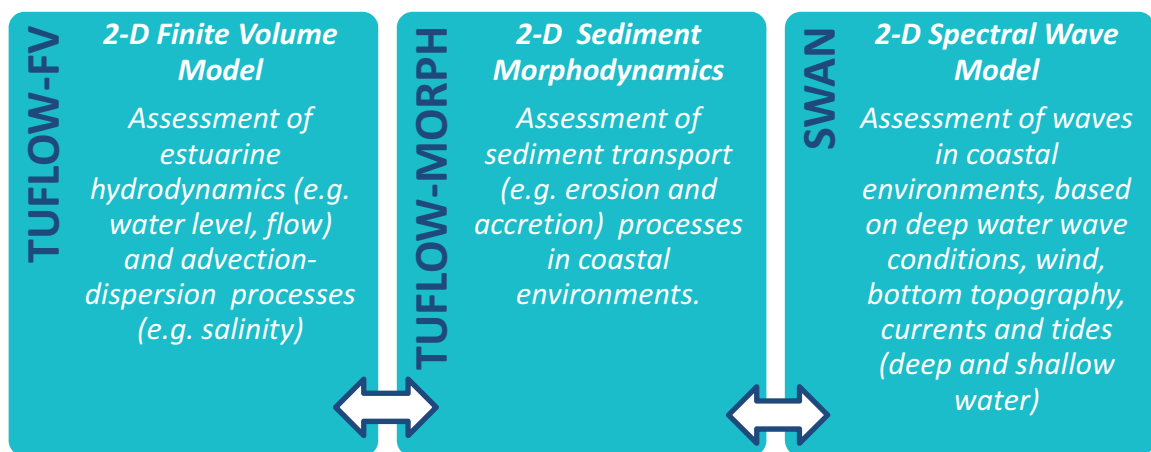


**Figure E-1 Numerical Models Adopted for the Investigations**

For numerical modelling investigations, tidal flows occurring within the study area are predicted by the hydrodynamic model (TUFLOW-FV) with the effect of waves introduced from the wave model (SWAN). Sediment supply to the entrance may result from the combined effects of waves and tidal flows. As waves approach the coast, they refract, diffract, shoal (rear up) and break. These processes generate forces which act to:

- Drive longshore currents; and
- Set up the water level at the shoreline.

In order to properly model coastal sediment transport processes, it is important to provide the resulting wave forces (also known as wave radiation stresses) to the hydrodynamic model. The waves also have a direct effect in stirring sediment from the bed and thus making it more available for transport by the currents. For this reason the spatial wave field needs to be supplied to the sand transport model (TUFLOW-MORPH) as well.

Using the numerical models outlined above, the overall morphological modelling process, including the effects that waves and tidal flows have on sediment transport, follow the structure outlined in Figure E-2. In all cases, the TUFLOW-FV hydrodynamic model is linked with the SWAN wave model, allowing the passage of wave stresses and the wave field to the hydrodynamic and sediment transport model, and bed elevations / current fields back to the wave model. This approach incorporates the important coastal processes occurring within the Estuary that influence its environmental condition and introduce changes to bathymetry over time.

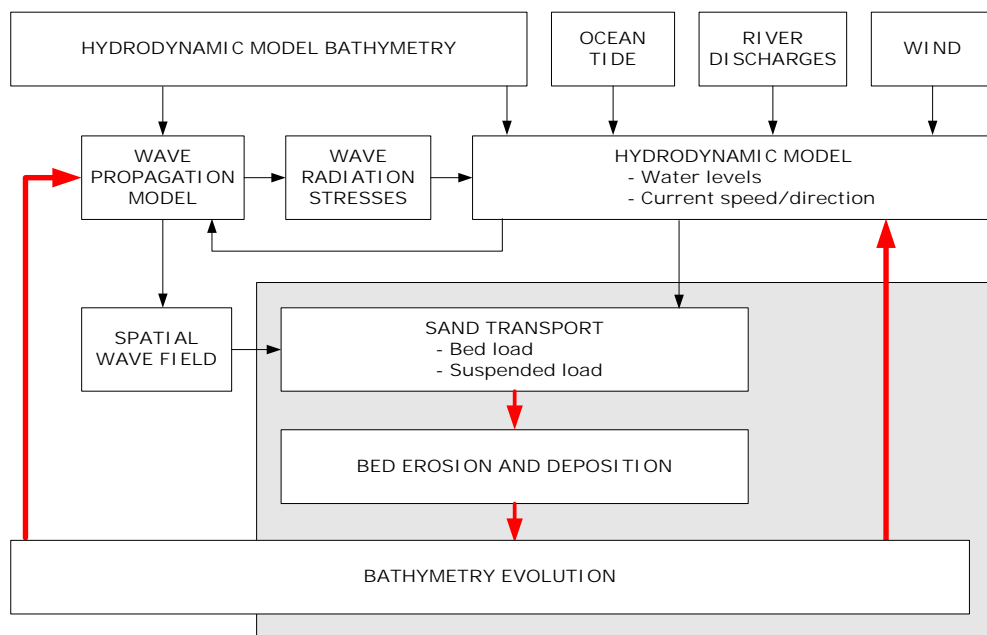


**Figure E-2 Combined Hydrodynamic, Wave and Morphological Modelling**

## E.2 Hydrodynamic modelling (TUFLOW-FV)

TUFLOW-FV is a two dimensional finite volume model code that solves the conservative integral form of the non-linear shallow water equations (NLSWE) (i.e. assuming that pressure varies hydrostatically with depth), including viscous flux terms and source terms for Coriolis force, bottom-friction and various surface and volume stresses. The model is currently fully operational as a 2-dimensional NLWSE solver, and development work to extend the model to a 3-dimensional NLSWE solver including baroclinic forcing is almost complete.

The scheme is also capable of simulating the advection and dispersion of multiple scalar constituents (e.g. salinity, temperature) within the model domain. Bed friction is modelled using a Manning’s roughness formulation and Coriolis force is also included in the model formulation. The spatial domain (or study area extents) is discretised using contiguous, non-overlapping irregular triangular and quadrilateral “cells”. Advantages of an irregular flexible mesh include:

- The ability to smoothly resolve bathymetric features of varying spatial scales (e.g. dredged channels adjacent to broad shoaled areas);
- The ability to smoothly and flexibly resolve boundaries such as coastlines; and
- The ability to adjust model resolution to suit the requirements of particular parts of the model domain without resorting to a “nesting” approach.

The flexible mesh approach has significant benefits when applied to study areas involving complex coastlines and embayments, varying bathymetries and sharply varying flow and scalar concentration gradients. TUFLOW-FV presently accommodates a wide variety of boundary conditions, including those necessary for modelling the processes of importance to the present study including water level and flow variations, wind stress and wave radiation stress, salinity and temperature. The assumption of a vertically well mixed water body means that the two-dimensional TUFLOW-FV is suitable. It is considered that three dimensional processes driven by salinity and / or thermal stratification are not significant issues for the study area, even though they might occur from time to time at some locations in response to fluvial inputs from the Myall Lakes. Sediment transport (erosion / accretion), water quality and tidal flushing are influenced by currents generated from a combination of tides and wave conditions and have been identified as the primary drivers influencing the issues of concern for the study area.

### E.2.1 Model Application

Figure E.2 shows the hydrodynamic model requires a combination of bathymetry, ocean tide, flow discharges, wind and wave stresses, as relevant, to calculate water level, current speed and direction. The transport and fate of constituents such as temperature and salinity (both conservative constituents) may also be included in a coupled advection-dispersion transport model. For the present study, salinity has been used as an indicator of flushing potential and expected water quality.

### E.2.2 Model geometry

The TUFLOW-FV numerical model geometry consists of nodes interconnected by a series of triangular and quadrilateral cells to form a two-dimensional mesh of the waterway system. The model geometry has been developed to capture the level of detail required to model important coastal estuarine processes while minimising model runtimes. The primary advantage of using a flexible mesh system is that it provides an accurate representation of the tidal prism without the need to define bathymetric conditions using a high resolution grid.

The model geometry includes the full tidal prism of the Port Stephens / Myall Lakes estuary with upstream extents defined by the tidal excursion limits of Tilligerry Creek, Myall River, Karuah River and the Bombah Broadwater. Furthermore, the entire Myall Lakes System is incorporated to represent the storage present in the system for simulations examining drainage of the Upper Lakes following a significant catchment runoff event. The model geometry includes increased detail to define the waterway areas of the Lower Myall River and channel connections in the vicinity of Corrie Island, i.e. the sand spit, the Northern Channel, Eastern Channel etc., which has been provided through increased spatial resolution where abrupt changes to bathymetry occur. Detailed geometry was extended upstream to ensure hydraulic properties of the Myall River are adequately represented by the model. The Lakes are located sufficiently upstream from the study area that a relatively coarse geometry is reasonable to capture the approximate storage property of the lake system.



For the remainder of the Port Stephens Estuary, the spatial resolution of model geometry was configured to capture other important bathymetric features including the shallow intertidal areas, tidal deltas and other flow connections present beyond the immediate study area. These are important to suitably represent tides propagating across the Port, towards the mouth of the Lower Myall River.

The model geometry was also extended beyond Yacaaba and Tomaree Headlands to include nearshore areas to a depth of approximately 50 metres which are important for ocean wave processes (i.e. wind and swell generated waves). The model geometry used to assess tidal hydrodynamics is shown in Figure E.3.

### E.2.3 Model bathymetry

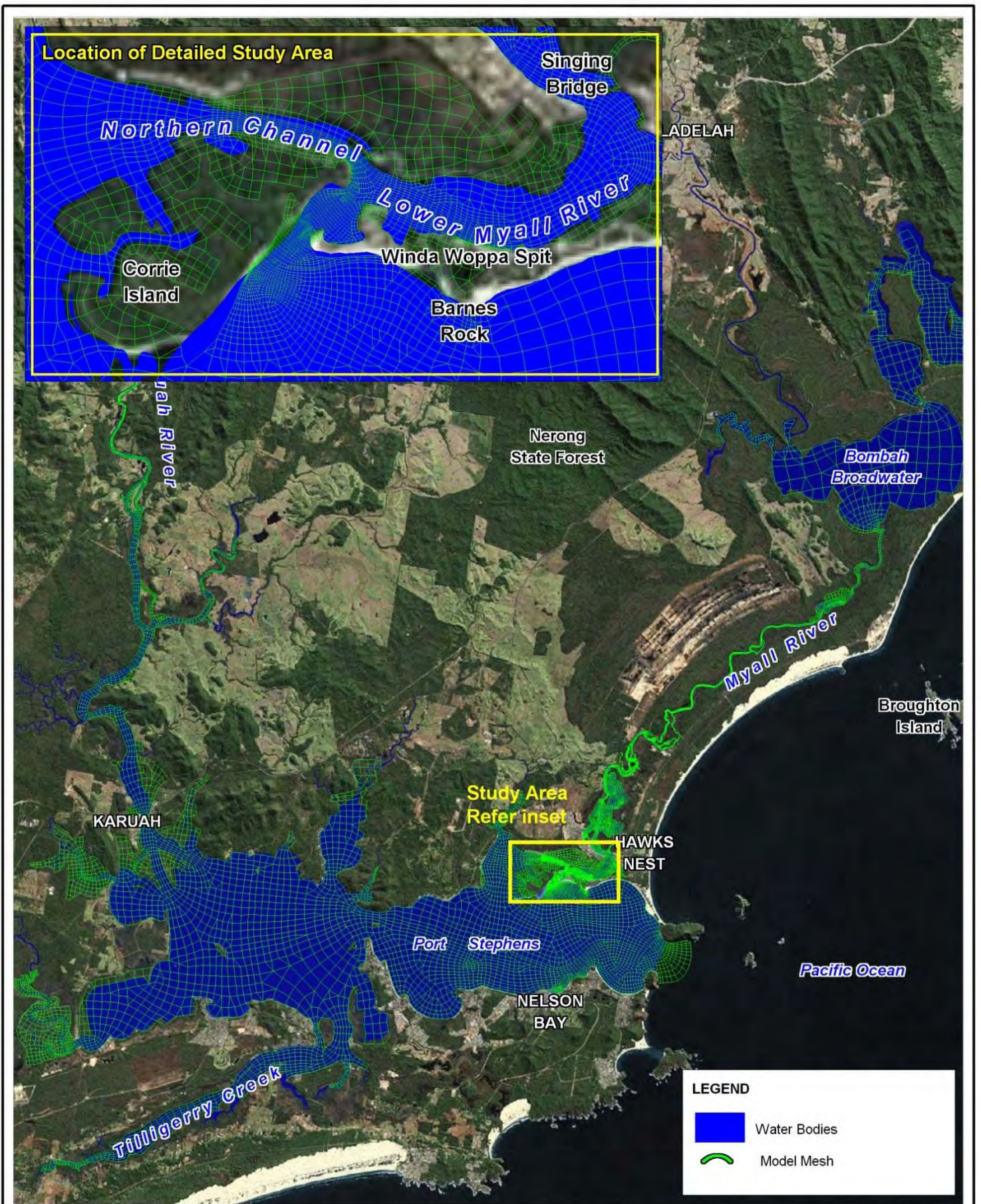
Hydrosurvey has previously been collected for the study area on a number of occasions (refer Section 3.1). The most recent data collection campaigns include hydrosurvey collected for the Myall River Entrance as part of the intensive tidal gauging exercise undertaken by DECCW in September 2009 and the more extensive hydrosurvey collected in 2001 which covers the eastern and central basin regions of Port Stephens. These two data sources form the basis of bathymetry data adopted by the numerical model along with additional hydrographic survey collected in 2001/2002 which has been incorporated to define bathymetric conditions for the Myall Lake (Bombah Broadwater) and the upper reaches of the Myall River.


Although these hydrosurvey data provide detailed coverage of the study area and a majority of the Port Stephens embayment, there are some locations west of study area that have not been covered by any previous data collection or survey campaigns, namely Tilligerry Creek, the western fringe of Port Stephens and Karuah River. A Digital Elevation Model (DEM) of bathymetric conditions derived from the various sources of hydrosurvey data has been refined with additional data sources including:

- Australian Hydrographic Service bathymetric chart (AUS809) of the western portion of Port Stephens absent from previous hydrosurvey;
- Light Detection And Ranging (LiDAR) data for definition of fringing saltmarsh and wetland overbank areas (i.e. inter-tidal areas beyond the extent of hydrosurvey with main channel that regularly wet and dry during a tidal cycle); and
- Rectified aerial photography to assist with definition and alignment of foreshore areas and extent of low lying vegetation species that are often associated with these low-lying intertidal areas.

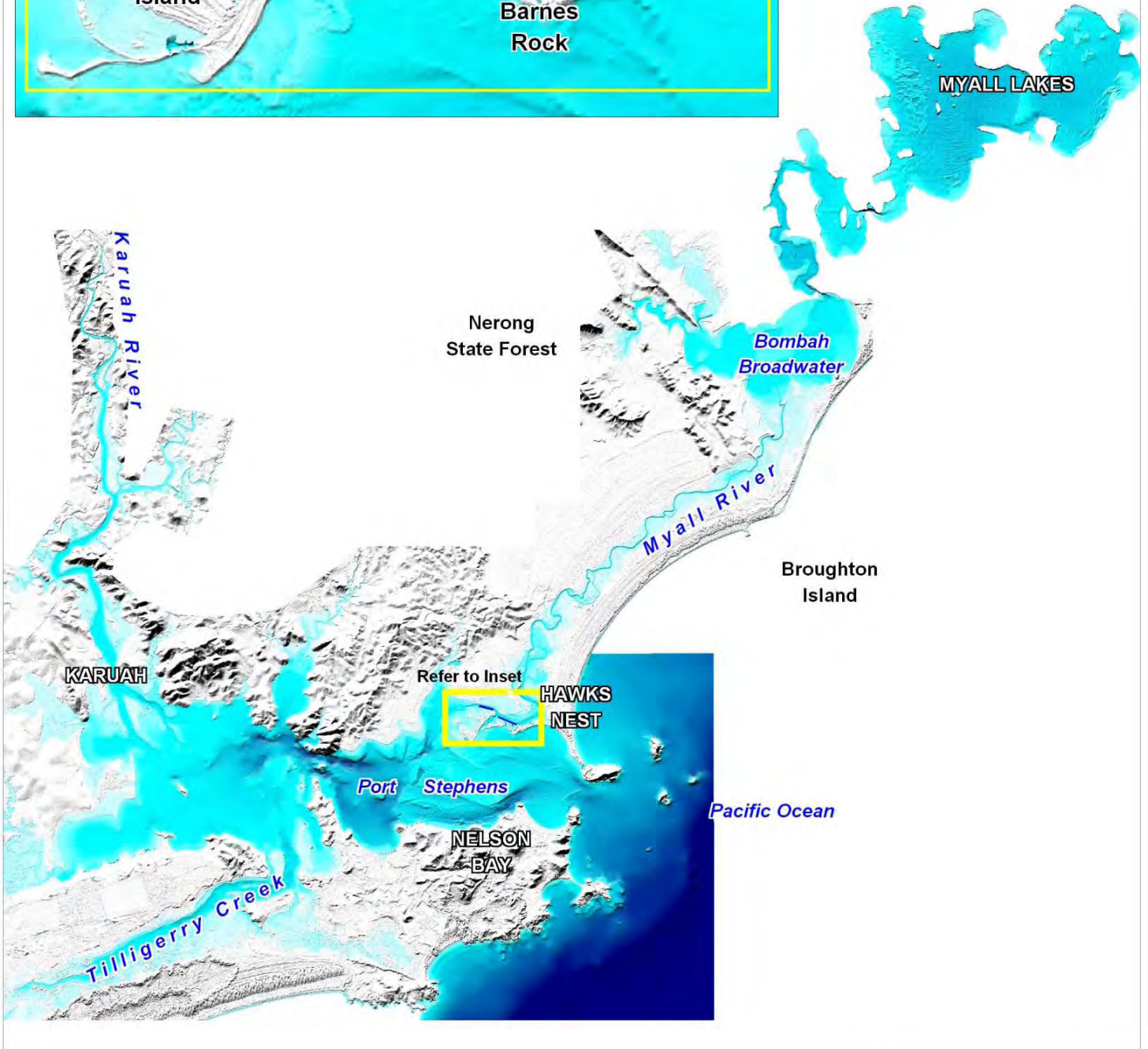
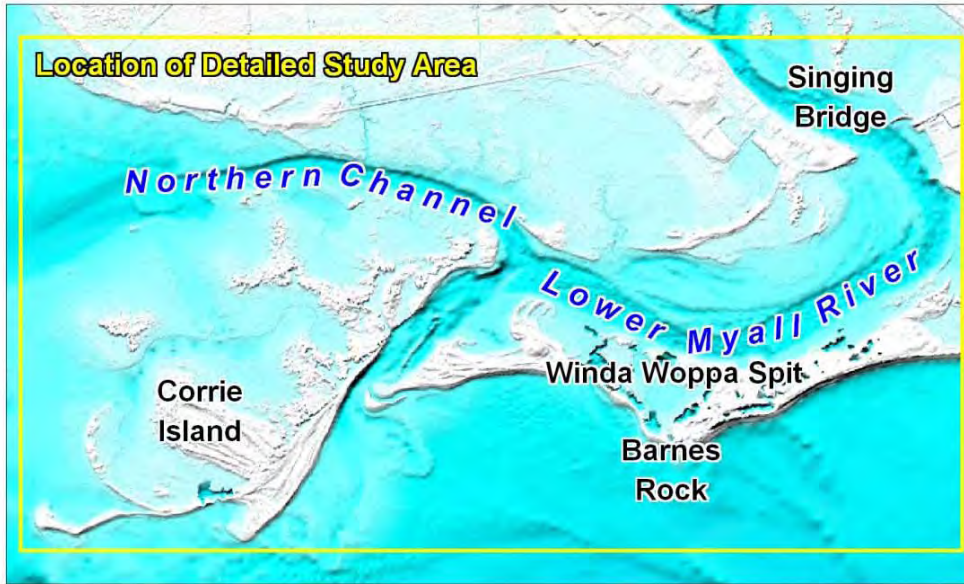
The hydrodynamic model was constructed to include the full tidal prism of the Port Stephens/ Myall Lake Estuary using the various bathymetry data sources described above. Areas seaward of entrance headlands were also included to account for the influence of waves propagating into the estuary. Bathymetry data for coastal / ocean areas seaward of the entrance was approximated by digitising depth contours from a 1:150,000 topographic chart (AUS00809 Port Jackson to Port Stephens derived from Australian Hydrographic Service). Ocean bathymetry in the vicinity of Port Stephens entrance was subsequently derived from digitised depth contours and incorporated within the DEM used to define bathymetry for the numerical model. The bathymetry used by the numerical model is shown in Figure E.4.





<p>Title:</p> <p><b>Model Mesh for Port Stephens and the Lower Myall River</b></p>	<p>Figure:</p> <p><b>E-3</b></p>	<p>Rev:</p> <p><b>A</b></p>
<p>BMT WBM endeavours to ensure that the information provided in this map is correct at the time of publication. BMT WBM does not warrant, guarantee or make representations regarding the currency and accuracy of information contained in this map.</p>	<p>0 5 10km</p> <p>Approx. Scale</p>	 <p>www.wbmpl.com.au</p>
<p>Filepath : K:\N1926_Lower_Myall_River_Sediment_Hydrodynamic_Assessment\MI\Workspaces\DRG_012_110202 Model Extents.WOR</p>		



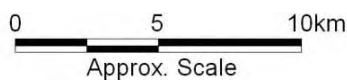


Title:  
**Hydrodynamic Model Bathymetry**

Figure:  
**E-4**

Rev:  
**A**

BMT WBM endeavours to ensure that the information provided in this map is correct at the time of publication. BMT WBM does not warrant, guarantee or make representations regarding the currency and accuracy of information contained in this map.



### E.2.4 Model configuration

The hydrodynamic model was configured to account for tidal hydrodynamics in response to tidal water level variations and wave stresses. The model was configured using the hydrostatic assumption (i.e. vertical momentum not solved) and depth averaged approximation of the governing Navier Stokes Equations. The influence of the Coriolis force was calculated with latitude of -32.7°S. Salinity was modelled as a passive transport scalar (i.e. uncoupled from temperature and density effects).

The scalar mixing model adopted was the Elder model which calculates non-isotropic diffusivity using coefficients for longitudinal and transverse directions. The momentum mixing model adopted was the Smagorinsky formulation with a coefficient of 0.2. TUFLOW-FV has an adaptive timestep algorithm which automatically adjusts the model timestep to resolve hydrodynamic and advection dispersion processes based on a user specified Courant-Friedrichs-Lewy (CFL) stability criterion.

TUFLOW-FV accounts for wetting and drying dynamically based of cell depths of 0.005 m and 0.05 m respectively. The drying value corresponds to a minimum depth below which the cell is dropped from computations (subject to the status of surrounding cells). The wet value corresponds to a minimum depth below which cell momentum is set to zero, in order to avoid unphysical velocities at very low depths. Bottom drag or bed roughness is specified as a spatially varying Manning’s *n* roughness value, which is standard for many two-dimensional hydrodynamic models.

### E.2.5 Boundary forcing

In order to simulate tidal hydrodynamics, a variable water level was applied to the ocean boundary to represent tide conditions. The water levels were those measured at the MHL ocean tide station at Tomaree. Recent measurements of ocean tide at Tomaree since January 2008 are presented in Figure E-5, which illustrates the occasional elevation of peak tidal water levels above normal astronomical tide levels (i.e. often peaks at ~ 1.2 m AHD, which is higher than peak astronomical tide levels of ~1.0 m AHD).

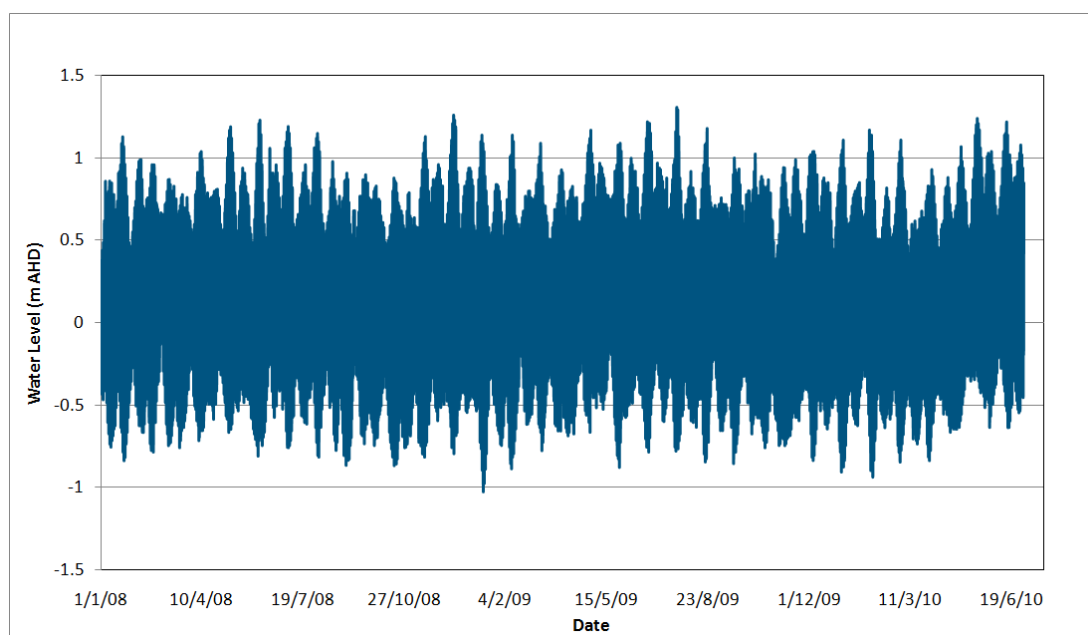


**Figure E-5 Ocean Tide Conditions, Port Stephens**



Where required, rainfall and evaporation were applied to the surface of the model explicitly as a global rate derived from the net daily rainfall and evaporation. No other boundary forcing (e.g. freshwater flows or groundwater) was applied to the model during stages of model development, calibration or scenario modelling. Separate boundary forcing data were however applied to the wave model and morphodynamic model, as discussed below.

### E.3 Wave modelling (SWAN)

The Simulating WAVes Nearshore (SWAN) model is a spectral coastal wave model code developed by the Technical University of Delft in the Netherlands.

The computer model developed for the Port Stephens / Myall Lakes Estuary adopts the SWAN spectral wave model to compute irregular waves in nearshore areas, based on variables such as deep water wave conditions, wind, bottom topography, currents and tides. SWAN may be configured to explicitly account for all relevant processes of propagation, generation by wind, interactions between the waves and decay by breaking and bottom friction with diffraction being included in an approximate manner (DHH, 2010).

Wave data, as represented by the significant wave height, period and mean direction of the two-dimensional wave spectrum is often required at coastal locations for coastal applications and modelling investigations. As discussed in Section E.1, the TUFLOW-FV hydrodynamic model is linked with the SWAN wave model to allow the passage of wave stresses to the hydrodynamic and sediment transport model to account for wave setup and longshore sediment transport, which influence the environmental condition and introduce changes to bathymetry within the Estuary.

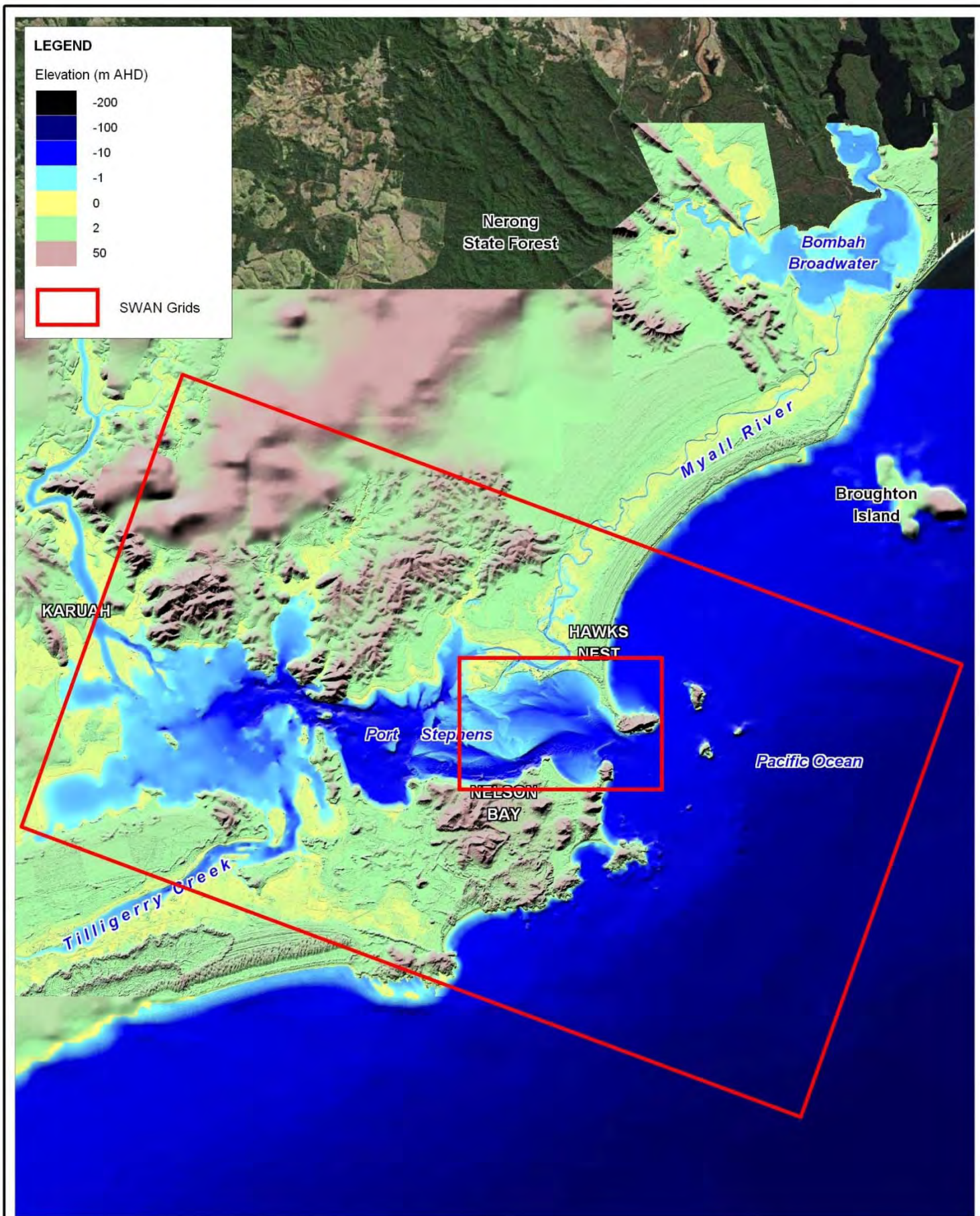
The wave model has been used to propagate “deep water” data measured at the WaveRider buoys inshore to the area of interest for the present study.

For the current study, a nonstationary two-dimensional SWAN model was developed to provide inputs to the hydrodynamic (TUFLOW-FV) and sediment transport (TUFLOW-MORPH) numerical models. Further details of the wave model development including bathymetry, geometry and boundary conditions are provided in the following sections.

#### E.3.1 Model geometry

The SWAN wave model consists of two grids, i.e. a coarse (larger) grid and a nested (smaller) grid with square cell sizes of 100 metres and 30 metres respectively. The extents of the coarse and nested grids are shown on Figure E-6

The purpose of the coarse grid wave model was to define offshore areas to a depth of approximately 100 metres (i.e. approximately 25 to 30 km from the coastline) to ensure that waves entered at the boundary were in similar depths to the waves measured at the WaveRider buoys. The coarse grid was orientated 70° in a counter clockwise direction from the positive (easterly) horizontal axis and was extended to the northern extent of Hawks Nest beach, as far south as Fingal Bay and as far west to cover all of Port Stephens.

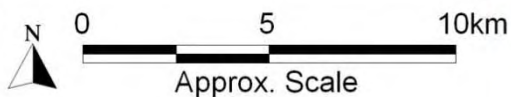


Title:  
**SWAN Model Grid extents**

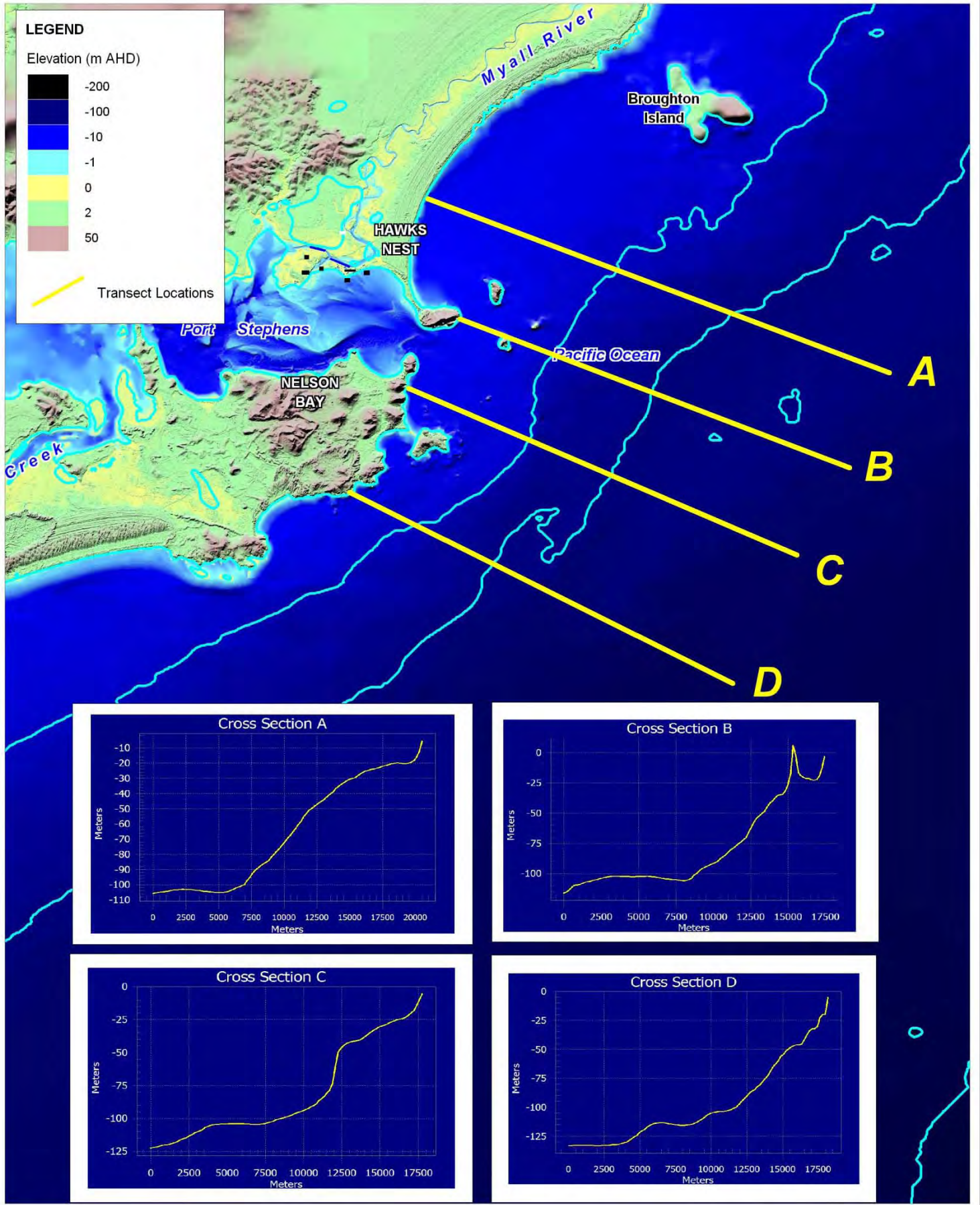
Figure:  
**E-6**

Rev:  
**A**

BMT WBM endeavours to ensure that the information provided in this map is correct at the time of publication. BMT WBM does not warrant, guarantee or make representations regarding the currency and accuracy of information contained in this map.







<p>Title: <b>Offshore Bathymetry Transects</b></p>		<p>Figure: <b>E-7</b></p>	<p>Rev: <b>A</b></p>
<p>BMT WBM endeavours to ensure that the information provided in this map is correct at the time of publication. BMT WBM does not warrant, guarantee or make representations regarding the currency and accuracy of information contained in this map.</p>			
<p>Filepath : K:\N1926_Lower_Myall_River_Sediment_Hydrodynamic_Assessment\MI\Workspaces\Figure 4-7 Offshore Bathymetry Profiles.WOR</p>			



The nested grid was used to calculate higher resolution wave information within the bounds of the hydrodynamic model. The nested grid covers the flood tide delta region of Port Stephens and was orientated such that the y-axis is aligned in the north-south direction and the x-axis aligned in the east-west direction (i.e. model grid was not rotated).

### E.3.2 Model bathymetry

Bathymetry or bottom topography required for development of the SWAN wave model includes ocean areas seaward of the entrance to a depth of approximately 100 metres. A DEM of nearshore and offshore bathymetry was estimated using depth contours digitised from a 1:150000 navigation chart for the east coast of Australia between Port Jackson and Port Stephens. These data were subsequently merged with other bathymetry data sources including that used for development of the hydrodynamic model to provide complete coverage for both wave model grids. The DEM of offshore bathymetry used by the SWAN wave model and some sample cross section profiles are shown in Figure E-7.

### E.3.3 Model configuration

SWAN models were run in a two dimensional and stationary (i.e. each computation of wave spectra is used as an initial condition for the next set of boundary conditions) mode. Processes included within the model were depth induced breaking (constant) and dissipation by bottom friction (using the standard friction Collins coefficient of 0.015). Spectral wave directions were only considered from the sector between 52° and 262° (i.e. the model only considers waves between the north-easterly and southerly aspects). The computation grid adopted for both coarse and nested grids was equivalent to the resolution and extents of the input bathymetric grid (i.e. no interpolation of bathymetry was required). Outputs from the model include, wave induced force, spectral peak period, peak wave direction, significant wave height and water depth.

### E.3.4 Boundary forcing

The WaveRider buoy data from Sydney were used as a boundary forcing for the coarse grid wave model, including temporal variations of significant wave height, wave period and wave direction. Wave data measured at Sydney for the period 1st to 30<sup>th</sup> September 2009 are shown in Figure 3-5, Figure 3-6 and Figure 3-7. In turn, the nested model was run interactively with TUFLOW-FV and used boundary conditions (i.e. wave spectra) calculated by the coarse wave model..

Local wind waves typically have shorter wave periods than ocean swell. It is generally accepted that waves of shorter period (for a given wave height) are more likely to be erosive, as the wave is steeper, and less affected by bottom friction as the wave approaches the shoreline due to its shorter wave period.

## E.4 Morphodynamic modelling (TUFLOW-MORPH)

The morphodynamic model, TUFLOW-MORPH, is an extension of the hydrodynamic model TUFLOW-FV (described in section). The morphodynamic component simulates patterns of sediment transport as governed by the hydrodynamics and applied boundary forcing. The processes and characteristics incorporated into the model include:

- Sediment transport and bed-evolution (sedimentation and erosion);

- Slumping of unstable slopes (both underwater and adjacent to water bodies);
- Sediment classes and ability to spatially vary sediment properties according to material type;
- Transport rates calculated using recent methods proposed by van Rijn's (van Rijn 2007a, 2007b, 2007c, 2007d); and
- Threshold velocity calculations using a shields criterion; and
- Option to calculate transport based on Particle size distribution parameters ( $D_{10}$ ,  $D_{50}$  and  $D_{90}$ ).

#### E.4.1 Model bathymetry

TUFLOW-Morph uses the same geometry as the TUFLOW-FV hydrodynamic model. The morphological model uses the same. The calculated sediment transport rates at each cell are applied within the finite volume scheme, utilising an upwind scheme to solve the sediment mass balance equation.

Sediment transport rates are calculated utilising a morphological time step which is larger than the hydrodynamic time step. Following testing, the morphological time step was set to 60 seconds.

While sediment transport is not calculated every hydraulic time step, the mass of sand within the bed is updated every time step. Consequently, the changes to bathymetry caused by erosion and scour have direct feedback to hydrodynamic processes every time step.

#### E.4.2 Model configuration

The morphodynamic model requires the input of sand grain sizes. The area of most significance to the study is located in and around the Eastern Channel. Section 3.6 provides data on sediments collected from the Myall. Based on that data the following sediment characteristics were applied in that area:

- $D_{10} = 0.16$  mm;
- $D_{50} = 0.41$  mm; and
- $D_{90} = 0.70$  mm;

While the sand in this area does moderately well sorted marine sands, there are some areas of known Coffee Rock (e.g. eastern edge of Corrie Island). It was assumed that the in-situ bed material had a dry density of  $1850 \text{ kg/m}^3$  (approximately equals sediment with a solid density of  $2650 \text{ kg/m}^3$  and a void ration of 0.4).

Currents generated by ocean tide and swell waves are used by the morphodynamic model to drive sediment transport processes. No other specific boundary forcing data are required by the morphodynamic model other than the initial model bathymetry.





**BMT WBM Brisbane**      Level 11, 490 Upper Edward Street Brisbane 4000  
PO Box 203 Spring Hill QLD 4004  
Tel +61 7 3831 6744 Fax +61 7 3832 3627  
Email [wbm@wbmpl.com.au](mailto:wbm@wbmpl.com.au)  
Web [www.wbmpl.com.au](http://www.wbmpl.com.au)

**BMT WBM Denver**      14 Inverness Drive East, #B132  
Englewood Denver Colorado 80112 USA  
Tel +1 303 792 9814 Fax +1 303 792 9742  
Email [wbm-denver@wbmpl.com.au](mailto:wbm-denver@wbmpl.com.au)  
Web [www.wbmpl.com.au](http://www.wbmpl.com.au)

**BMT WBM Melbourne**      Level 5, 99 King Street Melbourne 3000  
PO Box 604 Collins Street West VIC 8007  
Tel +61 3 9614 6400 Fax +61 3 9614 6966  
Email [wbm-melbourne@wbmpl.com.au](mailto:wbm-melbourne@wbmpl.com.au)  
Web [www.wbmpl.com.au](http://www.wbmpl.com.au)

**BMT WBM Morwell**      Cnr Hazelwood Drive & Miners Way Morwell 3840  
PO Box 888 Morwell VIC 3840  
Tel +61 3 5135 3400 Fax +61 3 5135 3444  
Email [wbm-morwell@wbmpl.com.au](mailto:wbm-morwell@wbmpl.com.au)  
Web [www.wbmpl.com.au](http://www.wbmpl.com.au)

**BMT WBM Newcastle**      126 Belford Street Broadmeadow 2292  
PO Box 266 Broadmeadow NSW 2292  
Tel +61 2 4940 8882 Fax +61 2 4940 8887  
Email [wbm-newcastle@wbmpl.com.au](mailto:wbm-newcastle@wbmpl.com.au)  
Web [www.wbmpl.com.au](http://www.wbmpl.com.au)

**BMT WBM Perth**      1 Brodie Hall Drive Technology Park Bentley 6102  
Tel +61 8 9328 2029 Fax +61 8 9486 7588  
Email [wbm-perth@wbmpl.com.au](mailto:wbm-perth@wbmpl.com.au)  
Web [www.wbmpl.com.au](http://www.wbmpl.com.au)

**BMT WBM Sydney**      Suite 206, 118 Great North Road Five Dock 2046  
PO Box 129 Five Dock NSW 2046  
Tel +61 2 9713 4836 Fax +61 2 9713 4890  
Email [wbm-sydney@wbmpl.com.au](mailto:wbm-sydney@wbmpl.com.au)  
Web [www.wbmpl.com.au](http://www.wbmpl.com.au)

**BMT WBM Vancouver**      1190 Melville Street #700 Vancouver  
British Columbia V6E 3W1 Canada  
Tel +1 604 683 5777 Fax +1 604 608 3232  
Email [wbm-vancouver@wbmpl.com.au](mailto:wbm-vancouver@wbmpl.com.au)  
Web [www.wbmpl.com.au](http://www.wbmpl.com.au)